

## Diagnosing infection of the CNS with MRI

MRI is an important tool in the diagnosis of CNS infections. It allows for identifying various infectious patterns, differentiates them from vascular pathologies or neoplasms, may raise suspicion about a specific pathogen agent and plays an important role in monitoring response to treatment. Recent advances in MRI (e.g., diffusion-weighted imaging and diffusion-tensor imaging, MR spectroscopy, susceptibility-weighted imaging and perfusion-weighted imaging) may further improve the specificity of the MR findings.

**KEYWORDS:** abscess ■ empyema ■ encephalitis ■ granuloma ■ infectious agents ■ MRI ■ myelitis

The CNS is relatively protected from infectious pathologies, owing to the presence of the axial skeleton, the meninges and the brain/spinal cord–blood barrier. Nonetheless, infectious agents may invade the CNS via the bloodstream, nervous fibers, direct spatial contiguity from sinonasal cavities, or directly after accidental or iatrogenic trauma. A large variety of infectious agents, including viruses, bacteria, fungi, parasites and prions, can gain access into the CNS, producing symptoms and clinical signs that are often nonspecific. Neuroimaging and biochemical tests play important roles in confirming the pathological process, localizing it, differentiating it from other pathologies (such as vascular or neoplastic) and identifying the etiologic agent.

MR imaging is the main radiological tool in diagnosing CNS infection due to the high anatomical resolution and tissue contrast, multiplanar acquisition and high sensitivity to contrast enhancement. More recent MR techniques, such as diffusion-weighted imaging (DWI), diffusion-tensor imaging (DTI), MR spectroscopy (MRS) and MR perfusion-weighted imaging (PWI) offer additional insight into the functional and metabolic features, further contributing to the understanding of pathological mechanisms of CNS infection [1].

### MR protocol

#### ■ Conventional MR sequences: T<sub>2</sub>, FLAIR, T<sub>1</sub> before & after gadolinium

The mainstays of MR protocol are the T<sub>2</sub>, T<sub>2</sub> fluid attenuated inversion recovery (FLAIR) and T<sub>1</sub> with gadolinium (Gd) chelates. The basic differentiation is extra-axial (i.e., outside the brain) versus intra-axial (i.e., inside the brain).

The latter may further be differentiated into, for example, ring-enhancing lesion, temporal lobe lesion, basal ganglia lesion and white matter abnormality [2].

Leptomeningeal involvement is typically not depicted on T<sub>2</sub> sequences, but it might be seen on FLAIR images (due to the presence of abnormal high protein cerebrospinal fluid [CSF] that is not nulled by the inversion–recovery pulse) or on T<sub>1</sub> Gd-enhanced images [3]. However, subarachnoid FLAIR hyperintensity is not specific for meningitis and has been described in various other conditions, such as subarachnoid hemorrhage, leptomeningeal metastasis, supplemental O<sub>2</sub> administration, intravenous anesthetic agents, or previous intravenous iodinated or Gd contrast material [4]. Several authors showed that Gd-enhanced FLAIR, especially delayed at approximately 20 min, improves the sensitivity of diagnosis of leptomeningeal infections due to the mild T<sub>1</sub> weighting of the FLAIR images [3,5,6]. The mechanism of leptomeningeal enhancement is breakdown of the blood–brain barrier without angiogenesis [7]. The contrast enhancement is typically thin and linear in viral and to a lesser extent also in bacterial meningitis, and it might be thicker or nodular in tuberculous or fungal meningitis. Enhancement along the cisternal segments of the cranial nerves is always abnormal and it might be encountered in infectious conditions, including viral meningitis [7] or neuroborreliosis [8], or noninfectious conditions, including granulomatous diseases, inflammatory demyelinating polyneuropathies, post-radiation neuritis or intracranial hypotension syndrome [2,9]. Also, leptomeningeal enhancement is not specific for infectious meningitis and

Victor Cuvinciu\*,  
Maria Isabel Vargas,  
Karl-Olof Lovblad  
& Sven Haller

Neuroradiology Department,  
University Hospitals of Geneva,  
4 rue Gabrielle-Perret-Gentil,  
1211 Geneva, Switzerland

\*Author for correspondence:

Tel.: +41 795532515

Fax: +41 223727072

victor.cuvinciu@hcuge.ch

can also be seen in leptomeningeal metastasis, neurosarcoidosis and chemical meningitis [2].

#### ■ $T_2^*$ weighted imaging gradient echo $T_2^*$ susceptibility weighted imaging

Gradient echo (GRE)  $T_2^*$  sequence is sensitive to the inhomogeneity of the magnetic field induced by paramagnetic substances, such as the decomposition products of hemoglobin or calcium. It is therefore of particular importance in the evaluation of possible herpetic encephalitis, abscess or neurocysticercosis. Susceptibility weighted imaging (SWI), a relatively new MR imaging sequence based on susceptibility differences between tissues, has been shown to be far superior to conventional  $T_2$  or GRE  $T_2^*$  sequences detecting microhemorrhages [10], and could thus be of potential value in cases of hemorrhagic infectious lesions.

#### ■ MR angiography: arterial and/or venous

Vascular sequences should be added in the MR protocol when there is a clinical or radiological suspicion of arterial or venous vascular involvement. Infectious vasculitis may complicate the evolution of meningitis (especially tuberculous meningitis), and may represent a cerebral complication of endocarditis (along with infective aneurysms) or of aspergillosis. Infectious venous thrombosis is a feared complication of sinusitis, otitis media or mastoiditis, especially in children [11].

#### ■ Diffusion imaging

DWI is sensitive to the brownian movement of water molecules that might be altered in various infectious processes. One parameter that influences the degree of diffusion weighting in DWI is the b-value, which depends on the strength, duration and timing of the diffusion-sensitizing gradients [12]. Conventional DWI uses b-values of 1000 s/mm<sup>2</sup>, but high b-value diffusion MR imaging (i.e., b = 3000 s/mm<sup>2</sup>) is more sensitive, due to the better signal intensity-to-noise ratio, better contrast-to-noise ratio and to the increased sensitivity to detect slowly diffusing water [12]. Restricted diffusion is due to the highly viscous proteinaceous fluid of pyogenic abscess [13], to the cytotoxic edema usually associated with irreversible neuronal damage of herpes virus encephalitis, or to the cytotoxic edema of the infected oligodendrocytes in progressive multifocal leukoencephalopathy (PML) [14]; sometimes, the mechanism is not very well understood, such as in Creutzfeldt–Jakob disease

where it could be related to the spongiform degeneration of the neuropil [15].

DTI is based on the anisotropic diffusion of water molecules that move more freely along the axon bundles as compared to perpendicular to the principal axonal direction. It allows for the quantification of tissue anisotropy, using parameters such as mean diffusivity (MD) and fractional anisotropy (FA), and it may depict white matter bundles (tractography). It is a promising technique that shows microstructural damage to the neuronal fibers before the changes become obvious with other MR sequences, such as in HIV patients [16,17] or subacute sclerosing panencephalitis [18,19].

#### ■ Perfusion weighted imaging

PWI estimates several microcirculatory parameters (mainly cerebral blood volume, cerebral blood flow and mean transit time). The most widely used method for analyzing brain masses is a  $T_2^*$ -weighted first-pass, dynamic susceptibility contrast-enhanced (DSC) method, which has an excellent signal-to-noise ratio and it is easily implemented, but is limited by the susceptibility artifacts of the skull base, hemorrhage, metals and gives semi-quantitative results. Perfusion parameter maps are reconstructed from dynamic data following the passage of a tracer (Gd chelates) through the cerebral vessels. Another method using exogenous tracer is  $T_1$ -weighted steady-state dynamic contrast-enhanced (DCE), with less susceptibility artifacts, offers quantitative results, but it has a weaker signal intensity in the brain [20,21]. A promising method is arterial-spin labeling (ASL), which uses magnetized blood as an endogenous tracer and measures the changes in tissue magnetization caused by the presence of labeled blood [21]. It has fewer artifacts than DSC perfusion, can be used in patients with renal failure and offers semiquantitative results [22]. At present it is mostly used in the research setting.

#### ■ MR spectroscopy

Proton MRS enables noninvasive *in vivo* quantification of normal and abnormal metabolite concentration in the brain. It has been proved to offer valuable complementary data to the classical MR protocol [23], assisting in the differential diagnosis of intracranial cystic lesions [24], granulomas [25] and encephalitis. MRS can be performed with either single voxel or multivoxel techniques. Single voxel spectroscopy offers the advantage of a good signal-to-noise ratio, easy implementation and relative rapid acquisition.

The main disadvantage is the reduced volume analyzed. This limitation was solved by multi-voxel spectroscopy, either 2D or 3D, that allows for the analysis of a larger volume, but with a lower signal-to-noise ratio and possible voxel contamination. Main metabolites identified are *N*-acetylaspartate (NAA; marker of neuronal viability), choline (marker of cellular membrane turnover), creatine (cerebral metabolism marker), myo-inositol (astrocyte marker), lactate (not present in the adult normal brain, indicates anaerobic glycolysis) and free lipids (necrosis).

### Imaging patterns in brain infection

Multiple imaging patterns are encountered in brain infections; for reviewing purposes, five basic patterns are described: extra-axial lesion, intra-axial ring-enhancing lesion, temporal lobe lesion, deep gray matter nuclei lesion and white matter abnormality [2].

#### ■ Extra-axial lesions

Extra-axial lesions include epidural empyema, subdural empyema and leptomeningitis; it is important to identify possible sources for infection (e.g., sinusitis, mastoiditis and otitis media) and complications (e.g., brain abscess, dural sinus thrombosis, infarction and hydrocephalus) [2]. In case of sinonasal inflammatory diseases with intracranial complications, it is of importance to complement the MR findings with CT, which can better depict osteolysis. The epidural empyema occurs between the calvarial inner table and the periosteum (which is actually the outer layer of the dura mater). Its expansion is limited by the tight connections between the bone and the periosteum and it is frequently paucysymptomatic, expressing mainly with headache. Its lenticular shape, without crossing the sutures, is similar to the epidural hematoma; the content is characteristically restricted on diffusion, with contrast enhancement of the dura. The subdural empyema has similar features of the content, but it extends freely in the subdural space and it manifests clinically with seizures, focal neurological deficits and coma [26].

#### ■ Intra-axial ring-enhancing lesion

Intra-axial ring-enhancing lesions are one of the most important imaging patterns in brain pathology; frequently, it is reduced to the basic question “neoplasm versus infection”, but important exceptions exist (demyelinating pathology, radionecrosis, subacute hematoma and subacute infarction) [2]. The infectious lesions tend to have a thin and regular rim of contrast

enhancement, while necrotic tumors have a thicker and irregular wall. A well-known sign for infectious lesions is the DWI hyperintensity of the content that favors the hypothesis of the pyogenic, tuberculous or even fungal abscess; this sign is not pathognomonic because it may also be encountered in hemorrhagic brain tumors. FA values might help further differentiate abscess from tumor in these confounding cases, with less overlap compared with DWI findings [27]. Note that some common infectious lesions do not regularly present with hyperintense central DWI, such as toxoplasmic abscesses or cysticercoid cysts.  $T_2$  and GRE  $T_2$  hypointensity of the wall suggest infection (due to free radicals induced by macrophage activation), but it is possible in tumors also (related to the hemorrhage, with ‘blooming effect’ on GRE  $T_2$ ). High-grade glial tumors might also be differentiated from abscesses from the analysis of the surrounding  $T_2$  hyperintensity; the infiltrative nature of these tumors is revealed by the increased rCBV [28] and choline [29], while the vasogenic edema related to infectious lesions should present with normal or low rCBV and normal choline.

#### ■ Intra-axial temporal lobe lesion

Intra-axial temporal lobe lesions include encephalitis (most notably herpes simplex encephalitis and Japanese encephalitis [JE]), infarction, infiltrating gliomas and limbic encephalitis [2]. In viral encephalitis, the clinical context (fever, headaches and seizures) and the imaging features (restricted diffusion and hypoperfusion) help the differential diagnosis.

#### ■ Intra-axial deep gray matter nuclei lesion

Intra-axial deep gray matter nuclei lesions include multiple vascular, neoplasm, metabolic causes, but also infectious (such as *Cryptococcus* pseudocysts, Creutzfeldt–Jakob disease). Bilaterally symmetric diffuse abnormalities involving entirely the basal ganglia suggest systemic or metabolic causes, while asymmetric or focal lesions involving partially the basal ganglia tend to indicate an infectious origin or neoplasms [30].

#### ■ Focal or diffuse white matter lesion

Focal or diffuse white matter lesion may be caused by various CNS infections, such as Lyme disease, HIV encephalopathy and PML. Owing to the variety of causes of leukoencephalopathy and to the often nonspecific imaging features, the clinical context, biological examinations

and, sometimes, even brain biopsy are necessary in order to confirm the diagnosis.

### Infectious diseases of the brain

#### ■ Bacterial infections

Bacterial infections may affect the CNS and any of the layers of meninges producing abscesses, ventriculitis, meningitis, subdural and epidural empyemas. Commonly, the imaging findings are nonspecific regarding the bacteria involved.

#### Brain abscess

Brain abscess is the most common focal infectious lesion in the CNS. It can originate from infection of contiguous structures (paranasal cavities, tympanic cavity and mastoid), secondary to hematogenous spread from distant sites (endocarditis), directly after accidental or iatrogenic trauma, and rarely following meningitis; in at least 15% of cases, no source can be identified [31]. Most abscesses occur at the gray–white matter junction. Initially there is an area of local cerebritis, visualized as a poorly demarcated area hyperintense on  $T_2$ -weighted images with little or no contrast enhancement. In the late cerebritis phase, an incomplete rim of enhancement is seen; in this phase, the antibiotic treatment alone can still stop the evolution, as the lack of a complete capsule allows for drug penetration [32]. Eventually, there may be a formation of a mature abscess; it presents with complete ring enhancement that is smooth, typically slightly thicker towards the gray matter due to the higher vascularization of the cortex. The thinner, internal part is susceptible of rupturing into the ventricular system, producing ventriculitis. The capsule is markedly hypointense on  $T_2$  images and it is surrounded by vasogenic edema. The hypointense  $T_2$  signal is thought to be secondary to the presence of paramagnetic free radicals inside the macrophages [33], responsible also for a slight  $T_1$  hyperintense signal. Hemorrhagic complications can be encountered, responsible for capsular or adjacent hematoma, rarely of isolated subarachnoid hemorrhage; the mechanism is probably due to the focal arteritis of the adjacent vessels [34]. The hemorrhagic complications are better depicted on GRE  $T_2^*$  as marked hypointensity with ‘blooming effect’. The extensive differential diagnosis of ring enhancing lesions is narrowed by the features on DWI of pyogenic abscesses, as they are quite invariably hyperintense with marked restriction of apparent diffusion coefficient (ADC) (FIGURE 1). The water restriction is related to the presence of pus, which consists of highly viscous proteinaceous fluid and numerous

white blood cells [35]. Nonetheless, this sign is not pathognomonic as cases of subacute hematomas and brain tumors with DWI hyperintensity and ADC restriction have been described [36]. These confounding cases might be further analyzed with DTI, since FA values are usually high in abscess cavity and much lower in neoplasm cysts with a cut-off value of 0.12–0.14 [27,37].

DWI is also important in evaluating the evolution after antibiotic treatment, as decreasing signal intensity on DWI trace and increasing ADC values correlate with a successful treatment; conversely, persistent or re-appearance of DWI trace hyperintensity signifies treatment failure [38]. MRS of pyogenic abscesses at TE of 135–144 ms shows cytosolic amino acids (0.9 ppm), lactate (inverted doublet at 1.33 ppm; FIGURE 1E), and inconstantly acetate (1.92 ppm) and succinate (2.4 ppm; not seen in our case), usually without detection of the normal brain metabolites (choline, creatine or NAA) if no partial volume effect is present. Loss of acetate and succinate peaks after treatment seems to correlate with a favorable evolution [39]. PWI is also of interest because the abscess wall is usually hypovascular, unlike the primary and secondary brain tumors that present with elevated rCBV [40].

#### TB

After decades of progressive decrease in developed countries, TB has seen resurgence for almost two decades because of the AIDS pandemic. The most common intracranial manifestation is meningitis, yet tuberculoma, abscess, vasculitis or ischemia can also be encountered. Tuberculous meningitis consists of a thick exudate, mainly in the basal cisterns, with leptomeningeal enhancement and FLAIR hyperintensity. Vasculitis (responsible of deep infarcts, FIGURE 2) and communicating hydrocephalus may complicate the disease. Intra-axial lesions (such as tuberculomas and tuberculous abscesses) form from hematogenous spread or direct extension from CSF via cortical veins or penetrating arterioles. The noncaseating tuberculoma is hypointense on  $T_2$ -weighted sequence with homogeneous enhancement and surrounded by vasogenic edema. The caseating tuberculoma is more heterogeneous, with peripheral contrast enhancement,  $T_2$  hypointensity and progressive increase in central  $T_2$  signal intensity, as the solid caseating necrosis becomes liquefied. After successful treatment, the lesions may calcify or even disappear [35,41]. The tuberculous abscess (FIGURE 3) has a higher bacterial load, is

more rapidly increasing and conventional imaging features are similar to pyogenic abscess. MRS might be used for differential diagnosis as the tuberculous abscess usually lacks the amino acids typical for pyogenic abscess [42].

### Neuroborreliosis

Neuroborreliosis (Lyme borreliosis) is a tick-transmitted multisystem inflammatory disease caused by *Borrelia* spirochetes [43]. The skin hallmark is erythema migrans, a migratory rash with a 'target' appearance. Neurologic manifestations are variable, including meningitis, radiculitis, cranial nerve palsies, encephalitis, myelitis and vasculitis [8]. White matter lesions resemble multiple sclerosis (MS) plaques, with periventricular, calloseseptal and arcuate U fibers involvement. The presence of contrast enhancement of the cranial nerves, of the leptomeninges and suggestive laboratory data favor the diagnosis of Lyme disease [8]; also, unlike MS, neuroborreliosis does not usually present with abnormalities on DTI and magnetization transfer ratios in normal-appearing white matter [44].

### ■ Viral infections

#### Herpes simplex encephalitis

Herpes simplex encephalitis (HSE) is a necrotizing, hemorrhagic meningoencephalitis, involving particularly the limbic system, especially the anteromesial temporal lobes, the insula, cingulate gyrus and the orbitofrontal region [35,45,46]. The presentation of HSE is rather nonspecific, but it should be suspected in patients with acutely deteriorating levels of consciousness, fever, abnormal CSF findings and focal neurological signs, in the absence of other causes [47]. The MRI is the imaging modality of choice, demonstrating lesions that are hyperintense on  $T_2$ , hypointense on  $T_1$ , frequently bilateral, yet unilateral involvement is not unusual (FIGURE 4). Contrast enhancement is not observed in the initial phases, but cortical gyral or meningeal enhancement can be observed with disease progression [48]. DWI is the most sensitive sequence for early detection of HSE, showing water restriction, compatible with cytotoxic edema. This cytotoxic edema is responsible for neuronal death in subacute and chronic stages, with subsequent increased extracellular space, increased water diffusibility and hypointensity on DWI trace [49]. This data is confirmed with DTI studies showing reduced MD and increased FA values in the earliest phases (suggesting cytotoxic edema), followed by increased MD and reduced FA (vasogenic edema) [50]. It seems that ADC

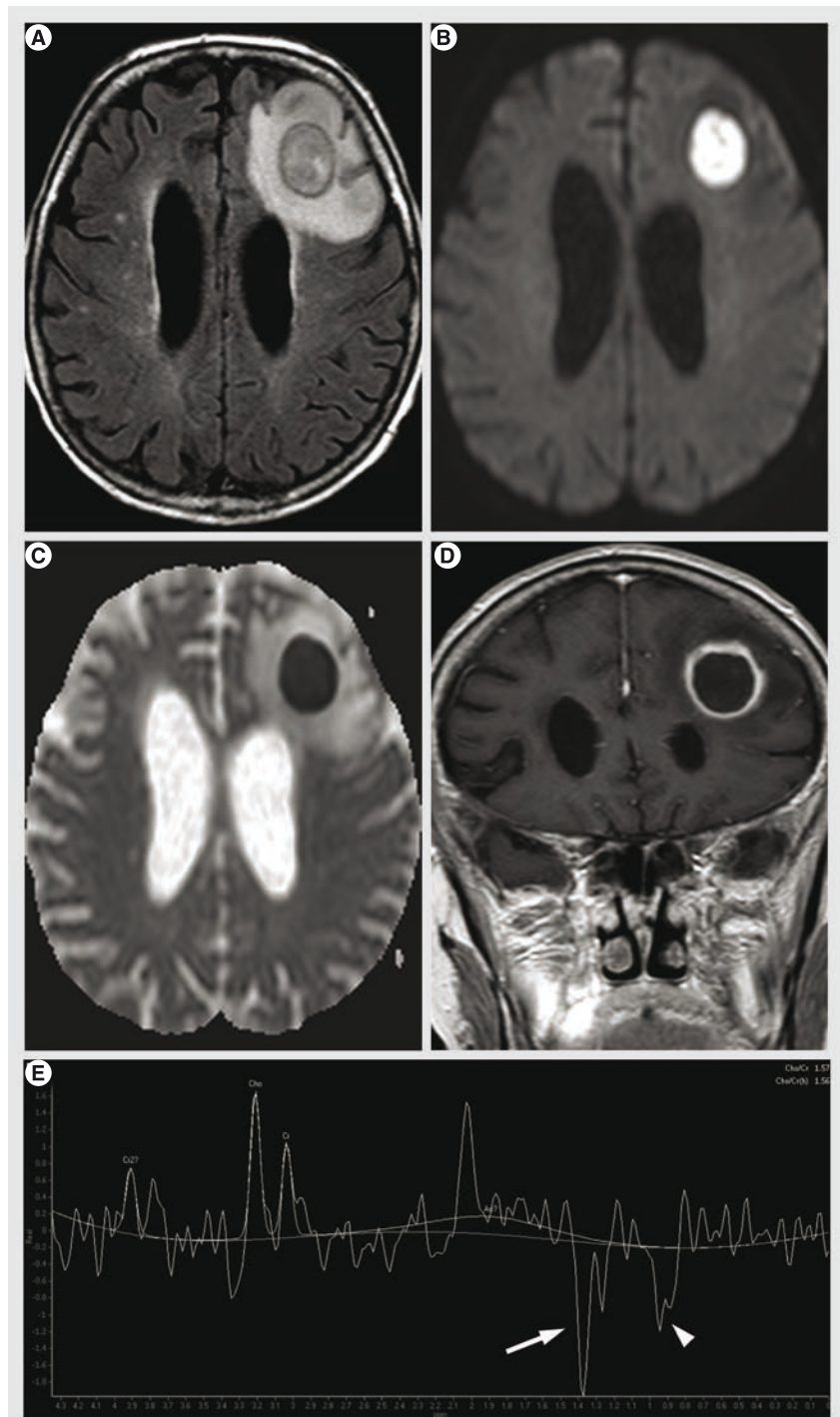


**Figure 1. Pyogenic abscess.** (A) Axial FLAIR image: left subcortical frontal cyst-appearing mass with hypointensity of the wall and surrounding edema. (B) Axial  $b = 1000 \text{ s/mm}^2$  of diffusion-weighted imaging: marked central hyperintensity. (C) Apparent diffusion coefficient map confirming the central water restriction and surrounding vasogenic edema. (D) Coronal gadolinium-enhanced  $T_1$  image showing the peripheral contrast enhancement; note also the thinner and smoother inner rim, toward the ventricular frontal horn. (E) Single voxel MR spectroscopy at TE 136 ms shows cytosolic amino acids (arrowhead) at 0.9 ppm and the inverted doublet of lactate (arrow) at 1.33 ppm; also, note the normal brain metabolites (increased choline and diminished *N*-acetylaspartate), due to the partial volume effect of the surrounding brain. The abscess was surgically evacuated and *Streptococcus* spp. was found at the biological examinations.

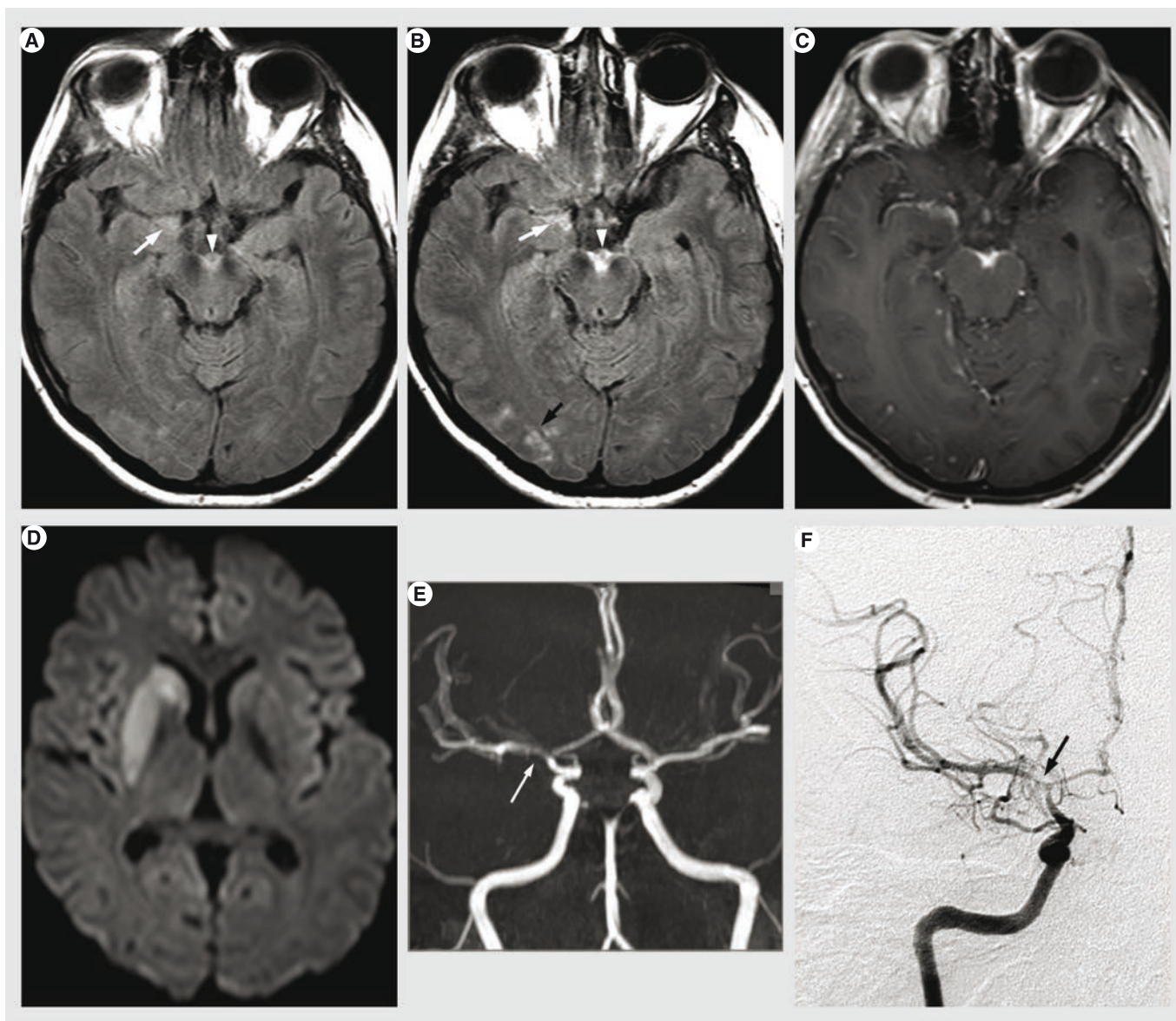


**Figure 2. Infarction and vasculitis complicating tuberculous meningitis.** (A) Axial FLAIR showing slight hyperintensity in the interpeduncular fossa (arrowhead) in the medial part of the right middle cerebral artery cistern (arrow). (B) Gadolinium-enhanced FLAIR better depicts the abnormality in the interpeduncular fossa (arrowhead) and middle cerebral artery cistern (white arrow) and it also clearly shows leptomenigeal enhancement in the right occipital lobe (black arrow). (C) Gadolinium-enhanced axial T<sub>1</sub>: leptomenigeal enhancement in the interpeduncular fossa and the internal part of the right middle cerebral artery cistern. (D) Axial b = 1000 s/mm<sup>2</sup> image: hyperintensity in the right striatum and the anterior limb of the internal capsule, suggesting deep middle cerebral artery infarction. (E) Antero-posterior maximum intensity projection of 3D time of flight angiography clearly showing thinning of the M1 segment of the right middle cerebral artery, at the origin of the lenticulostriate perforating arteries. (F) Antero-posterior projection of digital subtraction angiography confirming the MR angiography findings. *Mycobacterium tuberculosis* was identified in the cerebrospinal fluid.

values correlate with the clinical picture at presentation and with evolution, with higher values (less restriction) found with more benign clinical course [35]. The hemorrhage in HSE is mostly microscopic, and usually not seen on imaging, even on gradient echo T<sub>2</sub>\*; SWI sequence could possibly improve its detection due to the higher sensitivity for microbleeds [10], but its use could be limited by the susceptibility artifacts due to the proximity to the skull base. MRS shows

decreased NAA levels, increased choline levels and increased myo-inositol, but this pattern can also be encountered in low-grade infiltrative processes. In herpes encephalitis, rCBV is lower than the normal white matter, probably related to the alterations in blood-barrier function or decreased vascularity during the acute stage, and by reduced metabolism caused by neuronal death during the late course of the disease [47]. This finding might help to differentiate it

from infiltrative tumors, such as low-grade gliomas [47,51]; nonetheless, some low-grade gliomas might present with low rCBV.

The imaging differential diagnosis includes paraneoplastic limbic encephalitis (progressive evolution, no hemorrhage), status epilepticus (seizures, hyperperfusion, no hemorrhage), infarction (typical vascular distribution), low-grade glioma (progressive onset, without fever) and JE.

### Japanese encephalitis

JE is caused by a flavivirus that sporadically affects children and young adults in Asia, where it remains a major health problem because of the disabling neurologic deficits and high

fatality [52,53]. The typical imaging findings include bilateral thalamic, brainstem, cerebellum, cerebral cortex and basal ganglia lesions with hyper intensity on T<sub>2</sub>, frequently with hemorrhage; bilateral thalamic hemorrhage is considered highly specific for JE in an appropriate clinical context [35,53]. JE might also involve the temporal lobe, causing problems in differentiating it from HSE, but frequently it involves the body and the tail of the hippocampus, sparing the rest of the temporal lobe and the insula.

### Subacute sclerosing panencephalitis

Subacute sclerosing panencephalitis (SSPE) is a progressive neurodegenerative disorder caused

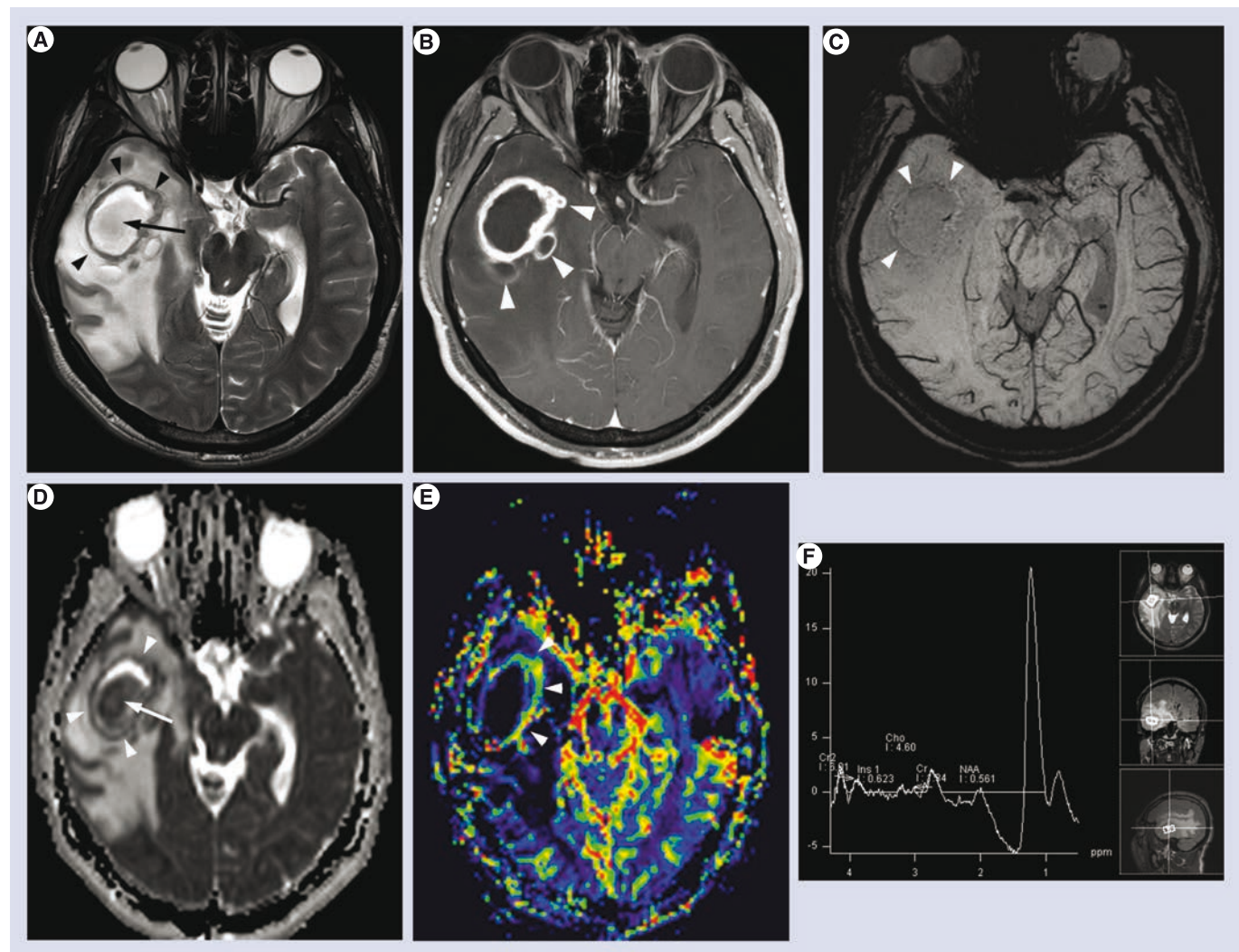


**Figure 3. Tuberculous abscess in an immunocompromised patient.** (A) Axial T<sub>2</sub> TSE image showing a right temporal heterogeneous cyst-like mass with hypointense wall (arrowheads) and a hypointense nodule (arrow). (B) Axial T<sub>1</sub> with gadolinium showing the intense contrast enhancement and better depicting the several peripheral cystic lesions (arrowheads). (C) Axial SWI: no susceptibility artifacts of the capsule (no sign of hemorrhage or calcification). (D) Apparent diffusion coefficient map showing low values of the wall (arrowheads) and the internal nodule (arrow). (E) Axial rCBV map showing the hypervascular capsule. (F) Monovoxel spectroscopy at TE 30 ms: high peak of lactate and free lipids, suggesting necrosis, but without metabolites in favor of pyogenic abscess (no significant peak at 0.9 ppm, 1.92 ppm or 2.4 ppm, suggesting cytosolic amino acids, acetate, and succinate respectively). The patient was operated and *Mycobacterium tuberculosis* was found at the pathological examination.

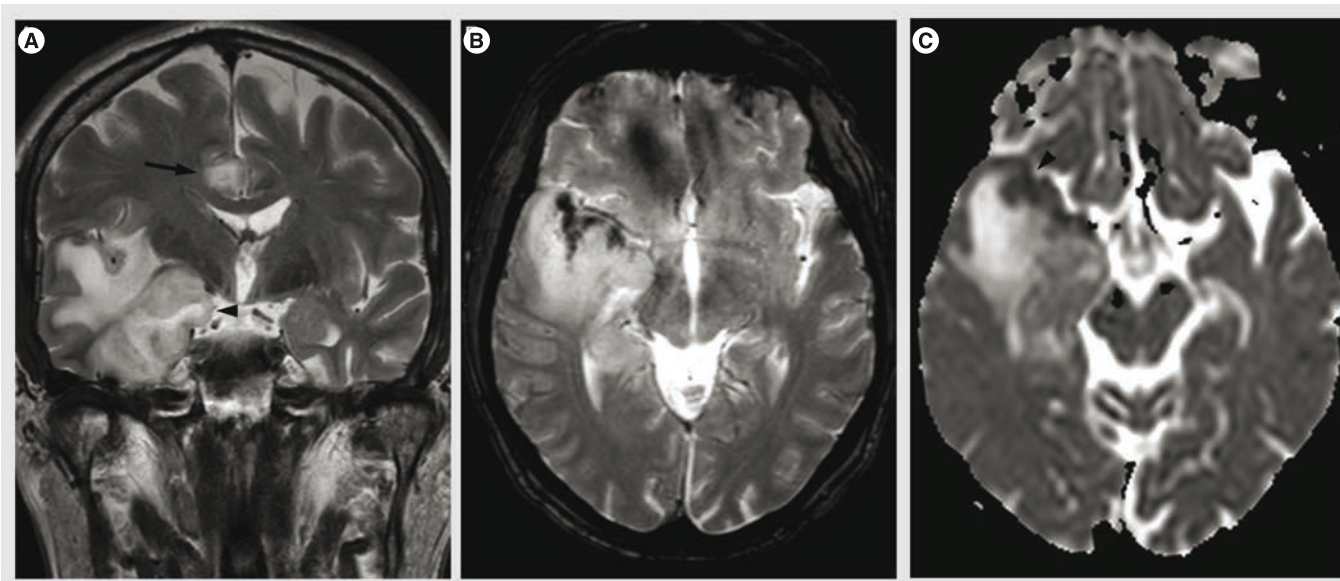


**Figure 4. Herpetic encephalitis.** (A) Coronal  $T_2$  image: hyperintensity of the right temporal lobe with mass effect and uncal herniation (arrowhead); note also the involvement of the right cingular gyrus (arrow). (B) Axial gradient echo  $T_2$  image: hypointensity of the anterior temporal cortex, in favor of hemorrhagic transformation. (C) Apparent diffusion coefficient map: reduced values in the anterior temporal cortex (arrowhead) and increased water diffusion in the subcortical white matter. PCR for herpes simplex virus type 1 was positive in the cerebrospinal fluid.

by a defective measles virus. Although its diagnosis is based on clinical findings, EEG and CSF features, MR imaging might be used to detect the demyelinating lesions. Initially, MR imaging shows  $T_2$  hyperintense lesions located preferentially in parietal and temporal lobes, that are subsequently extending into the periventricular white matter, corpus callosum and the basal ganglia; later, encephalomalacia and atrophy develop [54]. Conventional MR imaging correlates poorly with the clinicobiological grade of the disease [19]. Significant correlation between the clinical severity and absolute concentrations of NAA and myoinositol spectroscopy were described in frontal normal-appearing white matter [55]. DWI studies have also reported increased ADC values in normal-appearing white matter compared with controls [56]. Also, DTI studies show reduced mean FA in major white matter tracts of patients with SSPE compared with healthy controls, with a significant inverse correlation of mean FA with clinical grades [19].

#### HIV infection

HIV infection often involves the brain, either directly or through opportunistic infections or neoplasms. Primary HIV infection is the most frequent CNS abnormality in HIV-positive patients in developed countries, where antiretroviral therapy is widely available; in more resource-limited countries, CNS opportunistic infections remain prevalent [41]. Primary HIV infection expresses with HIV dementia complex,

a chronic neurodegenerative syndrome characterized by progressive cognitive and motor impairment and brain atrophy. The imaging findings are referred to as HIV encephalopathy and they are represented by cerebral atrophy and periventricular, bilateral  $T_2$  hyperintensities, isointense or slightly hypointense on  $T_1$  images, with increased ADC, without involvement of the subcortical arcuate U fibers, without mass effect or contrast enhancement. In the presence of mass effect and/or contrast enhancement, other diagnostic methods should be considered [41]. After highly active antiretroviral treatment, the  $T_2$  hyperintense abnormalities in the white matter may improve. MR is less sensitive than histopathological studies in showing the real extent of the white matter lesions, but MRS and DTI offer promising results, showing abnormalities in normal-appearing brain; MRS demonstrates moderately diminished NAA and increased choline levels, while DTI depicts diminished FA in the splenium of corpus callosum and subcortical white matter, more important in patients with the most advanced HIV infection [16].

#### Progressive multifocal leukoencephalopathy

PML is a demyelinating disease caused by reactivation of JC virus in immune deficiency conditions (HIV infection, lymphoma, immunosuppressive or immunomodulating therapy) [57]. Histopathologically, it is characterized by

extensive and progressive demyelination with notable absence of significant inflammatory response [58]. MRI shows single or multifocal asymmetric white matter T<sub>2</sub> hyperintensities, with T<sub>1</sub> hypointensity, with mild or without mass effect or contrast enhancement. It may also involve gray matter; hemorrhage is uncommon,

but possible. New lesions and the advancing edge of large lesions present with DWI hyperintensity with diminished ADC, interpreted as the cytotoxic edema of active infection and proved as oligodendrocyte swelling on pathology [14,58]. Older lesions and the center of large lesions have increased ADC values, related to

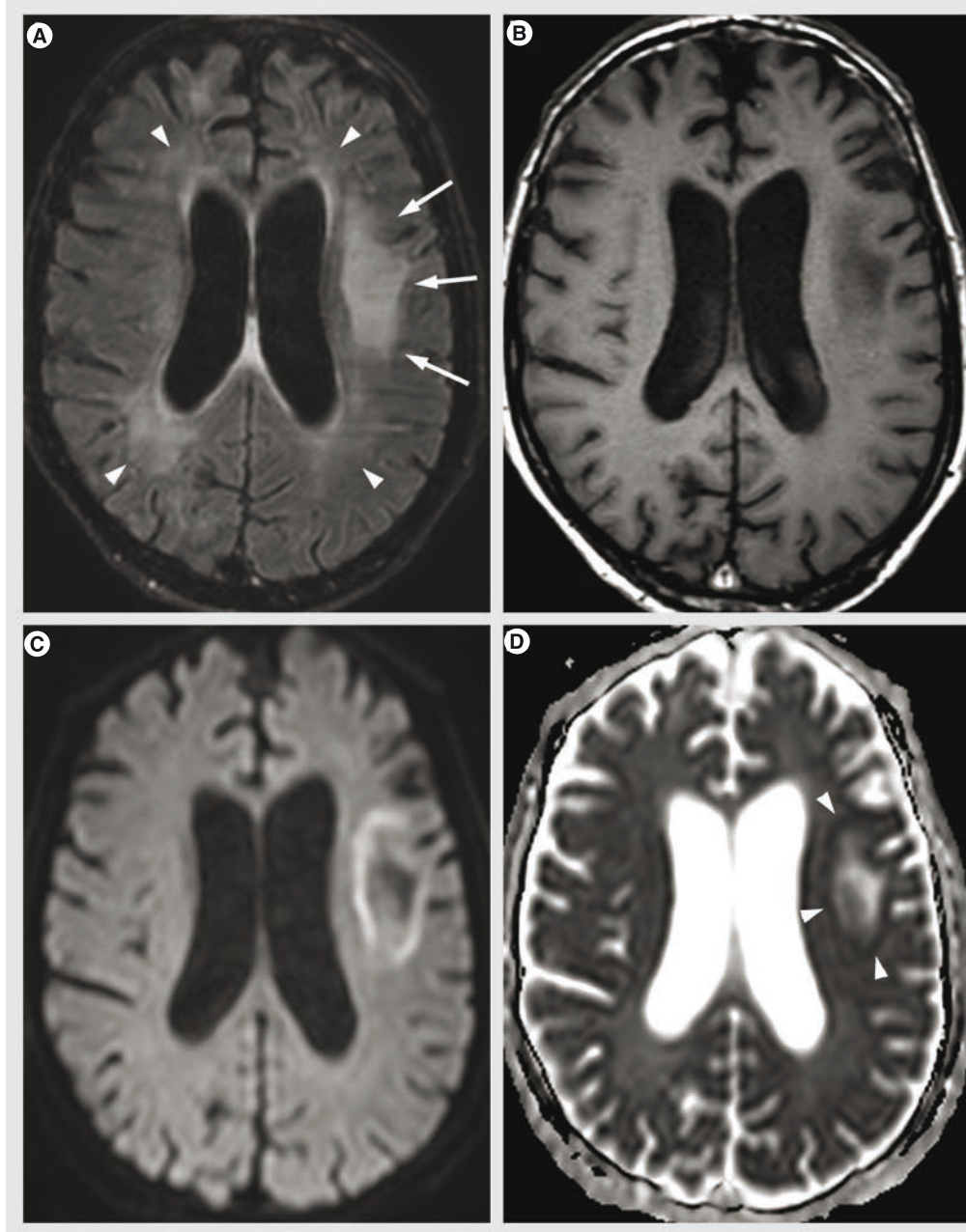


**Figure 5. Progressive multifocal leukoencephalopathy and possible HIV encephalopathy.** (A) Axial reconstruction of 3D FLAIR showing left subcortical hyperintensity without mass effect (white arrows) compatible with progressive multifocal leukoencephalopathy and periventricular bilateral hyperintensities (arrowheads) suggesting HIV encephalopathy. (B) Axial T<sub>1</sub> image showing hypointensity of progressive multifocal leukoencephalopathy and isointensity of HIV encephalopathy. (C) Axial b = 1000 s/mm<sup>2</sup> diffusion image: hyperintense rim of progressive multifocal leukoencephalopathy. (D) Axial apparent diffusion coefficient map confirming the peripheral water restriction (arrowheads). JC virus DNA was identified in the cerebrospinal fluid; no pathological confirmation for HIV encephalopathy was obtained.

the increased extracellular space secondary to dead oligodendrocytes and astrocytic reparative processes [14]. This heterogeneity can also be confirmed with proton MRS that shows different metabolite patterns in newer versus older lesions, with higher increase of choline and lower decrease of NAA in newer lesions, suggesting the ongoing demyelination without the severe neural or axonal loss that appears afterwards [59]. The differential diagnosis with HIV encephalopathy is based on the asymmetrical white matter lesions,  $T_1$  hypointensity, peripheral involvement (from the subcortical arcuate fibers towards deep white matter) and the DWI features (FIGURE 5).

### Cytomegalovirus

Cytomegalovirus is an opportunistic herpes virus that remains in latent form in the general population and reactivates in the setting of immune suppression. It can produce meningoencephalitis, ventriculitis, myelitis, polyradiculitis and retinitis [41]. MRI is often normal and, when positive, it is often nonspecific with atrophy and diffuse hyperintensities on  $T_2$ -weighted images. A more specific pattern is thin, linear periventricular enhancement, suggesting ependymitis; the differential diagnosis includes bacterial ventriculitis (intraventricular DWI hyperintense content) and lymphoma (nodular, irregular enhancement) [35,41].

## ■ Parasitic infections

### Toxoplasma

Toxoplasma is an ubiquitous intracellular parasite that produces latent infection in a wide range of normal populations; its activation occurs in immunosuppressive conditions, mostly in AIDS patients [41], when the  $CD4$  counts reach less than 100 cells/ $\mu$ l. Toxoplasmosis results in a necrotizing encephalitis, seen on MR imaging as multiple areas of  $T_2$  hyperintensities, with nodular or ring-like enhancement surrounded by vasogenic edema (FIGURE 6). Hemorrhage is rare, but it may help in the differential diagnosis with lymphoma that does not typically bleed before treatment [41]. Another sign that is highly suggestive of toxoplasmosis is the 'eccentric target sign' (FIGURE 6D), a small enhancing nodule within and adjacent to the enhancing ring [60].

The two most frequent brain mass lesions in HIV patients, toxoplasmosis and lymphoma, have very similar imaging features. On metabolic imaging (thallium-201 brain SPECT, FDG-PET) lymphoma is positive, whereas toxoplasmosis is not; SPECT is considered very

accurate for masses over 2 cm [61]. MR perfusion shows increased relative cerebral blood volume in lymphoma, whereas the toxoplasmosis lesions are hypovascular [62]. MRS shows an increased choline peak for lymphoma; if the analysis is inadvertently made in the tumoral necrosis, the spectra will contain high peaks of lipids and lactate, similar to the toxoplasmic lesions [41]. Lymphoma is usually hyperintense on DWI trace, due to its high cellularity, but its value in the differential diagnosis is limited by the heterogeneous characteristics of DWI trace in toxoplasmosis [63]. Frequently, a follow-up after toxoplasmosis treatment is necessary to differentiate between toxoplasmosis versus lymphoma, but it is important to notice that lymphoma may temporarily diminish due to the corticosteroid treatment that accompanies the antitoxoplasmosis regimens [35]. After healing, the toxoplasma lesions may disappear completely or leave calcified sequelae.

### Cysticercosis

Cysticercosis is the most frequent cerebral parasitosis in immunocompetent patients and it is a major cause of acquired epilepsy in most low-income countries. It is produced by ingesting the eggs of *Taenia solium*, with subsequent hematogenous spread and brain contamination. In the brain, the parasites present with multiple stages:

- The vesicular stage: with thin-walled cysts located at the cortical–subcortical junction, without edema, with minimal or no contrast enhancement; it is possible to identify the scolex as a small nodular structure within and adjacent to the wall ('cyst with a dot' image); the liquid content has a CSF-like appearance;
- Colloidal stage: after release of antigens and immune response, there is an increasing edema and contrast enhancement, and the content of the cyst is hyperintense on FLAIR images and with increased diffusion;
- Granular stage: the lesion presents as an involuting nodule with contrast enhancement and mild edema;
- Calcified nodular stage: without contrast enhancement or edema [35,64].

A specific type of neurocysticercosis is the racemose form (FIGURE 7), with multiple, loculated cysts, without visible scolex or contrast enhancement, located mainly in the basal cisterns and ventricular system, and producing obstructive hydrocephalus. Their detection is

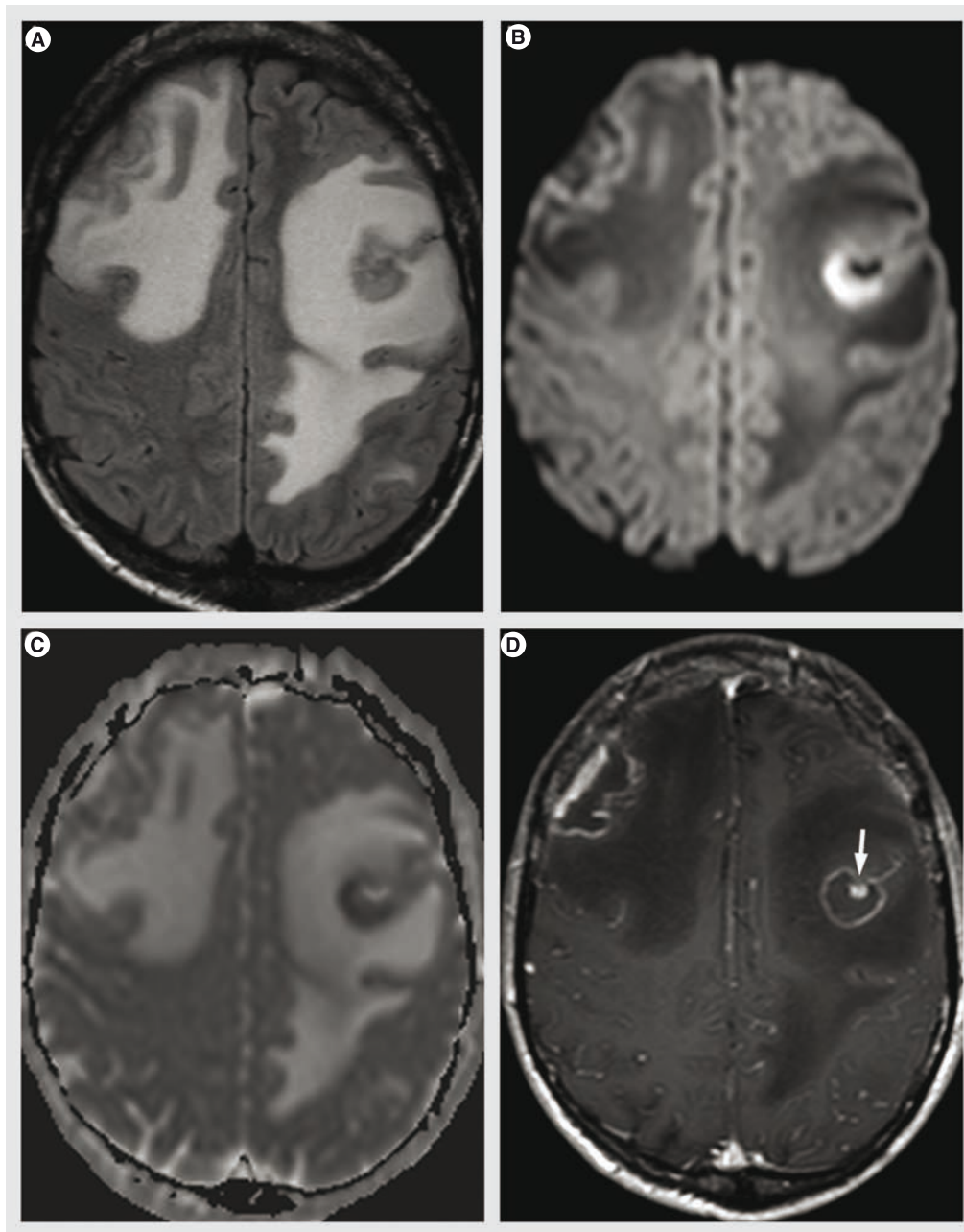


**Figure 6. Toxoplasmosis in an immunocompromised patient.** (A) Axial FLAIR image showing bilateral frontal lesions surrounded by vast areas of hyperintensities suggesting vasogenic edema. (B) Axial  $b = 1000 \text{ s/mm}^2$  image: hyperintense left frontal lesion; note that the right frontal lesion is isointense on diffusion-weighted imaging. (C) Apparent diffusion coefficient map confirming water restriction in the left frontal lesion. (D) Axial gadolinium-enhanced  $T_1$  shows the two frontal lesions with peripheral irregular enhancing rim; note the left lesion presents the 'eccentric target sign' (arrow), strongly suggestive of the diagnosis. The patient presented with favorable evolution after the anti-toxoplasmosis regimen.

improved by using heavily weighted 3D T2 images or FLAIR after inhalation of 100% oxygen that produces hyperintensity of the CSF and better visualization of the cyst wall [65].

#### ■ Fungal infections

Fungal infections are rare, but life threatening, and they occur mainly in diabetic or

immunocompromised patients. The most common species encountered are *Aspergillus*, *Candida* and *Cryptococcus*.

#### *Cryptococcus*

*Cryptococcus* is the most common fungal infection of the CNS in AIDS, occurring in 5–10% of patients [35]. It spreads hematogenously from

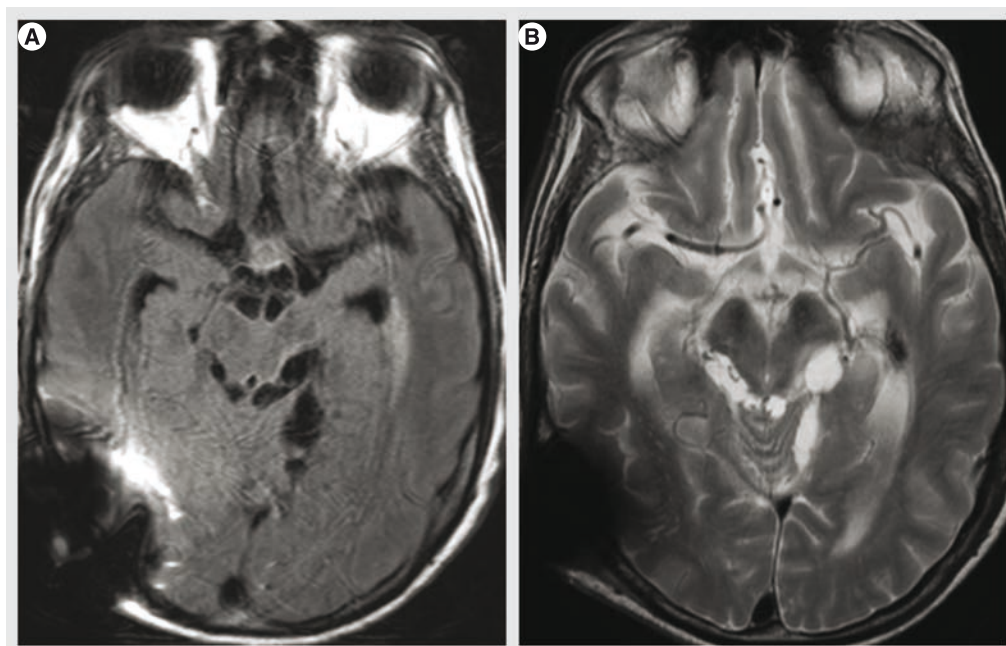


**Figure 7. Racemose cysticercosis.** Axial FLAIR (A) and T<sub>2</sub> (B) showing multiple cyst-like lesions in the basal cisterns; the right temporo-occipital hypointense image is an artifact induced by the ventriculo-peritoneal derivation valve for hydrocephalus.

the lung to the CNS. It may manifest with meningitis, meningoencephalitis, hydrocephalus, gelatinous pseudocysts, intraventricular or intraparenchymal cryptococcomas [35,41]. Gelatinous pseudocysts are dilated perivascular spaces due to *Cryptococcus* spreading from the basal cisterns; they appear on imaging as rapidly growing, nonenhancing ‘cysts’. Cryptococcomas are rare; usually they have a relatively low T<sub>2</sub> signal, with nodular or ring-like enhancement, without specific features differentiating them from granulomas of other origin (FIGURE 8); it is rather the topography of the granulomas of the choroid plexus that is characteristic for cryptococcosis [66].

#### *Aspergillus*

*Aspergillus* species are ubiquitous fungi that enter the body through the respiratory system and gain access to the brain hematogenously or via the paranasal sinuses. Cerebral aspergillosis has a poor prognosis in immunocompromised patients, with a mortality approaching 100% [67]. *Aspergillus* is angioinvasive, with a predilection for perforating arteries, resulting in ischemia, hemorrhage, infectious cerebritis and abscess [62,67]. Cerebritis is seen as disseminated areas of T<sub>2</sub> and FLAIR hyperintensity with minimal or no contrast enhancement. Abscesses are ring-enhancing lesions, with capsular T<sub>2</sub> hypointensity and central DWI hyperintensity. T<sub>2</sub> hypointensity is related to hemorrhage and

the presence of iron, manganese and magnesium in the fungal concretions [68]. The central DWI hyperintensity is caused by the restricted diffusion of water in the presence of coagulative necrosis and polymorphonuclear cells [69]. The diagnostic differential with other fungal infections or with pyogenic and tuberculous abscesses is very difficult; the presence of hemorrhage in immunocompromised patients should raise the suspicion of aspergillosis [41].

#### ■ Prion diseases

Prion diseases are characterized by brain deposition of an aberrant form of a constitutively formed protein (abnormally folded, protease-resistant isoform of a normal cellular protein termed ‘PrP<sup>C</sup>’); prions are considered infectious agents because of their heritable and self-perpetuating nature, even if they do not require cotransmission of nucleic acid [70]. The best known of prion diseases is the Creutzfeldt–Jakob disease (CJD), with several forms (sporadic, inherited familial form and variant form, which is considered transmissible and has been associated with bovine spongiform encephalopathy) [71]. The clinical picture includes rapidly progressive dementia associated with myoclonic jerks and akinetic mutism. The characteristic EEG shows continuous periodic sharp waves [72] and the analysis of CSF is performed in search for 14-3-3 protein, a surrogate biomarker for CJD [73]. The MR diagnosis is strongly supported by FLAIR

hyperintensity with restricted diffusion within the cortex and striatum, with or without thalamic abnormalities; 'the pulvinar sign', defined by increased intensity of the pulvinar relative to

the anterior putamen, is noted in the majority of variant CJD patients [74]. High b-value diffusion MR imaging (i.e.,  $b = 3000 \text{ s/mm}^2$ ), is more sensitive than conventional DWI (that uses b-values

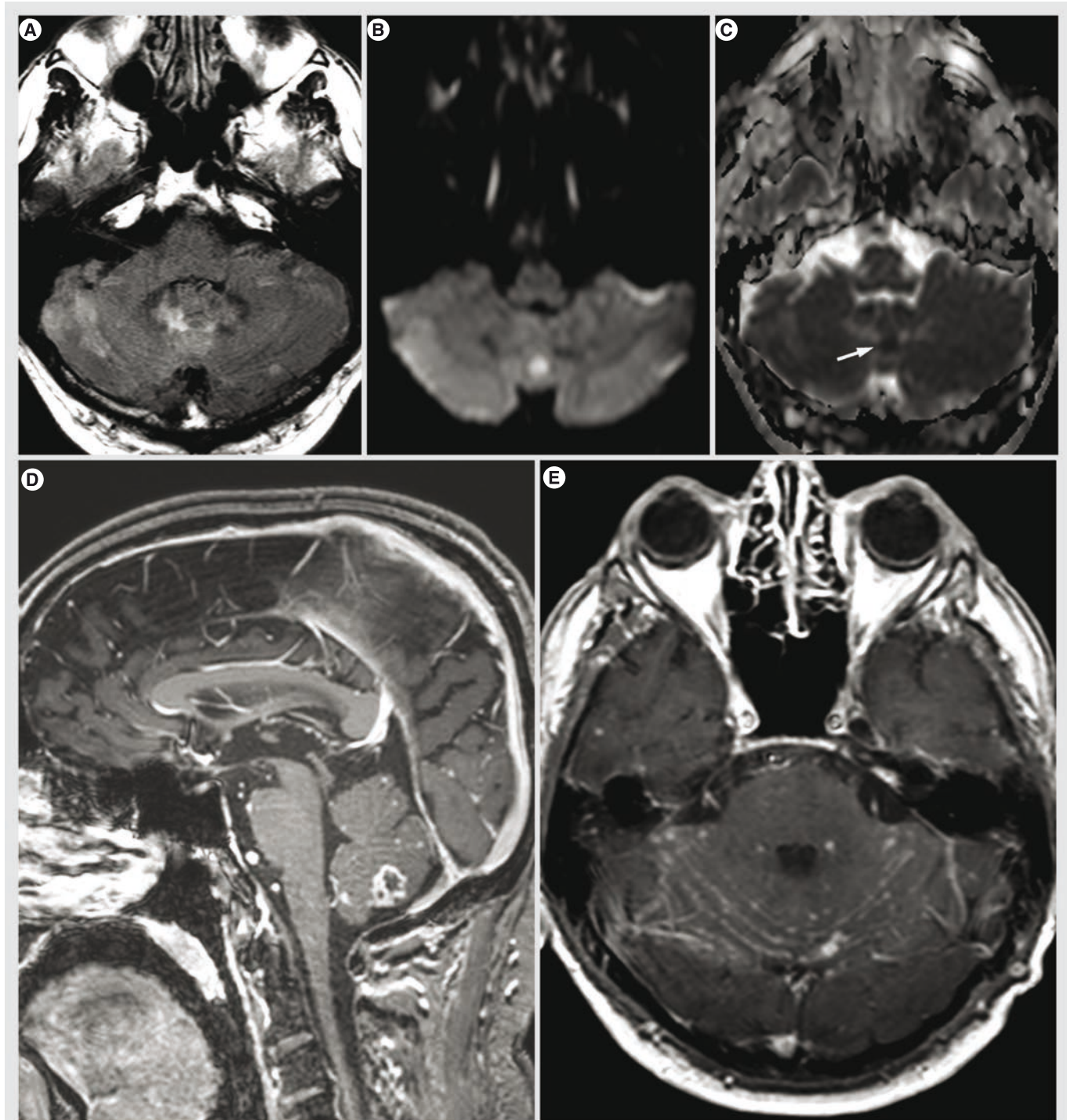


**Figure 8. *Cryptococcus* infection in an immunocompromised patient.** (A) Axial FLAIR image shows multiple patchy hyperintensities in the posterior fossa. (B) Axial  $b = 1000 \text{ s/mm}^2$  showing focal cerebellar hyperintensity. (C) Apparent diffusion coefficient map confirming the water restriction (arrow). (D) Sagittal gadolinium-enhanced 3D  $T_1$ ; cerebellar lesion with irregular peripheral enhancement (cryptococcoma) and multiple punctate superficial lesions. (E) Axial gadolinium-enhanced  $T_1$  showing irregular leptomeningeal contrast enhancement and multiple punctate superficial lesions (possibly small cryptococcomas). Encapsulated yeasts of *Cryptococcus neoformans* were identified in the direct examination of cerebrospinal fluid, after China ink coloration.

of 1000 s/mm<sup>2</sup>), and it might be used in clinical conditions when the findings are equivocal on low b-value DWI [12]. FLAIR hyperintensity with the same topography, but without diffusion abnormalities in the initial phase, is considered as atypical for CJD and suggests another diagnosis [74]. The restricted diffusion is suspected to be related to the spongiform degeneration of the neuropil [15]. Advanced disease with more severe cell loss and rarefaction of the extracellular compartment is accompanied by reduction of the DWI signal intensity and pseudonormalization and even elevation of ADC values [75].

#### ■ Varia

##### Meningitis

Meningitis is an inflammatory reaction of the meninges, of bacterial, viral or fungal origin. The diagnosis is based on the clinical picture, with headache, fever, neck stiffness, photophobia, vomiting and altered consciousness [35]. Imaging is not usually indicated, unless the clinical presentation is atypical, there is clinical suspicion of increased intracranial pressure or if a complication is suspected. The imaging signs of increased intracranial pressure are coning (descent of cerebellar tonsils and brainstem through the foramen magnum), effaced cerebellar cisterns, cerebellar reversal sign, effaced ventricles and cortical sulci [32]. Lumbar puncture should be performed if no contraindication is present. Cerebrospinal fluid in aseptic meningitis, usually due to viral causes, presents with elevated white blood cell count with lymphocytic predominance, normal or increased proteins, normal glucose and low lactic acid. In bacterial meningitis, the CSF analysis shows elevated white blood cell count with neutrophilic predominance, increased proteins, decreased glucose, decreased CSF–blood glucose ratio and increased lactate [76].

Leptomeningeal inflammation might be seen on FLAIR, delayed Gd-enhanced FLAIR or Gd-enhanced T<sub>1</sub> sequences. In acute meningitis, the inflammation is preferentially located over the cerebral convexity, whereas in chronic meningitis as seen with TB or fungi, the enhancement is more evident in the basal cisterns [35]. The contrast enhancement is thin and linear in bacterial and viral meningitis, and it can be thicker or nodular in fungal and tuberculous meningitis [7].

The most common complications are hydrocephalus, sterile subdural effusions, subdural empyemas, vasculitis, infarcts and ventriculitis. Due to the purulent content, the empyemas have

diffusion features similar to the brain abscesses, with hyperintensity on DWI trace and diminished ADC; the sterile collections have similar intensity with CSF [77]. Peripheral contrast enhancement is also noted in subdural or epidural empyemas. Brain parenchyma adjacent to the subdural empyemas often presents with reactive vasogenic edema that may complicate with cerebritis. Ventriculitis is rarely isolated and usually complicates meningitis, abscess or shunting, and increases mortality to 80%. Imaging features include enhancement of the ventricular wall and hyperintense ventricular content on DWI trace [2].

##### Immune reconstitution inflammatory syndrome

Immune reconstitution inflammatory syndrome (IRIS) is a clinical aggravation in immunocompromised patients that present a biological improvement after immune recovery. It is caused by the newly acquired capacity of the immune system to mount an inflammatory response against opportunistic infectious agents that were previously tolerated. In HIV infection, it can appear after combined antiretroviral therapy [78]. Multiple infectious agents may be involved, the most frequent in the CNS being JC virus, herpes simplex virus, HIV, *Mycobacterium*, *Cryptococcus* and *Toxoplasma*. Rapid extension of T<sub>2</sub> hyperintensities, marked contrast enhancement and mass effect are MR features suggesting PML-IRIS (FIGURE 9). DWI was used for assessing the initial response of PML to combined antiretroviral therapy [79]. The preliminary results seem to indicate that patients with higher ADC values at the center of the lesions are at risk of developing PML-IRIS, possibly due to the more extensive demyelination and more advanced initial disease. Also, MRS in PML-IRIS shows a higher increase of choline, lactate and free lipids peak compared to PML, with relatively stable NAA, compatible with increased inflammatory response [80]. For other opportunistic agents, the imaging features lack specificity, but MR has a supportive role for the clinicobiological diagnosis of IRIS and is used to monitor the evolution.

##### Systemic infections

Systemic infections might also present with neurological impairment needing further exploration by MR imaging. Intracranial abnormalities occur in 30–50% of patients with infective endocarditis during the course of the disease and are often detected before infective endocarditis

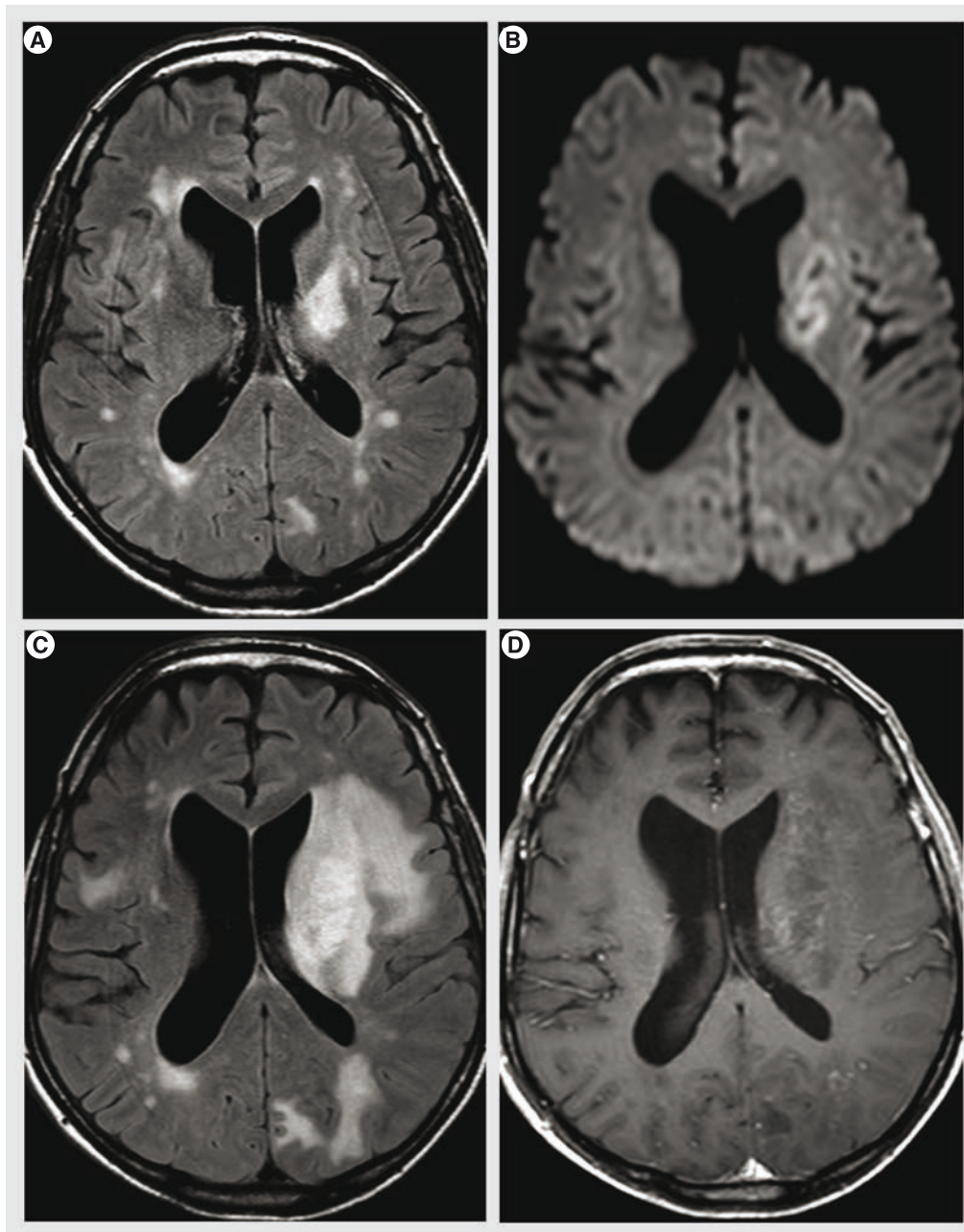


**Figure 9. Progressive multifocal leukoencephalopathy-associated immune reconstitution inflammatory syndrome in a HIV-positive patient. (A)** Axial FLAIR image showing left capsulo-lenticular hyperintensity suggesting progressive multifocal leukoencephalopathy; note also multiple hyperintensities of the subcortical and periventricular white matter of lesser specificity. **(B)**  $b = 1000 \text{ s/mm}^2$  image of diffusion-weighted imaging: peripheral hyperintensity rim. **(C)** After 2 months of antiretroviral treatment, with good biological response, but paradoxical clinical aggravation, axial FLAIR image reveals a marked increase in size and mass effect appearance. **(D)** Axial gadolinium-enhanced  $T_1$  image shows patchy contrast enhancement; note also the left subcortical frontal and parietal punctate contrast enhancement, suggesting other areas of progressive multifocal leukoencephalopathy-immune reconstitution inflammatory syndrome.

is diagnosed [81]. The mechanism is bacterial thromboembolism and proliferation, and various lesions might be encountered, such as cerebritis, abscess, meningitis, ischemia, hemorrhage, vasculitis, infectious aneurysms and venous thrombosis (FIGURE 10).

In sepsis, the brain may be affected by many systemic disturbances, such as hypotension, hypoxemia, hyperglycemia and hypoglycemia, or by direct brain pathologies, such as ischemic brain lesions, cerebral micro- and macro-hemorrhage, abscesses, posterior reversible

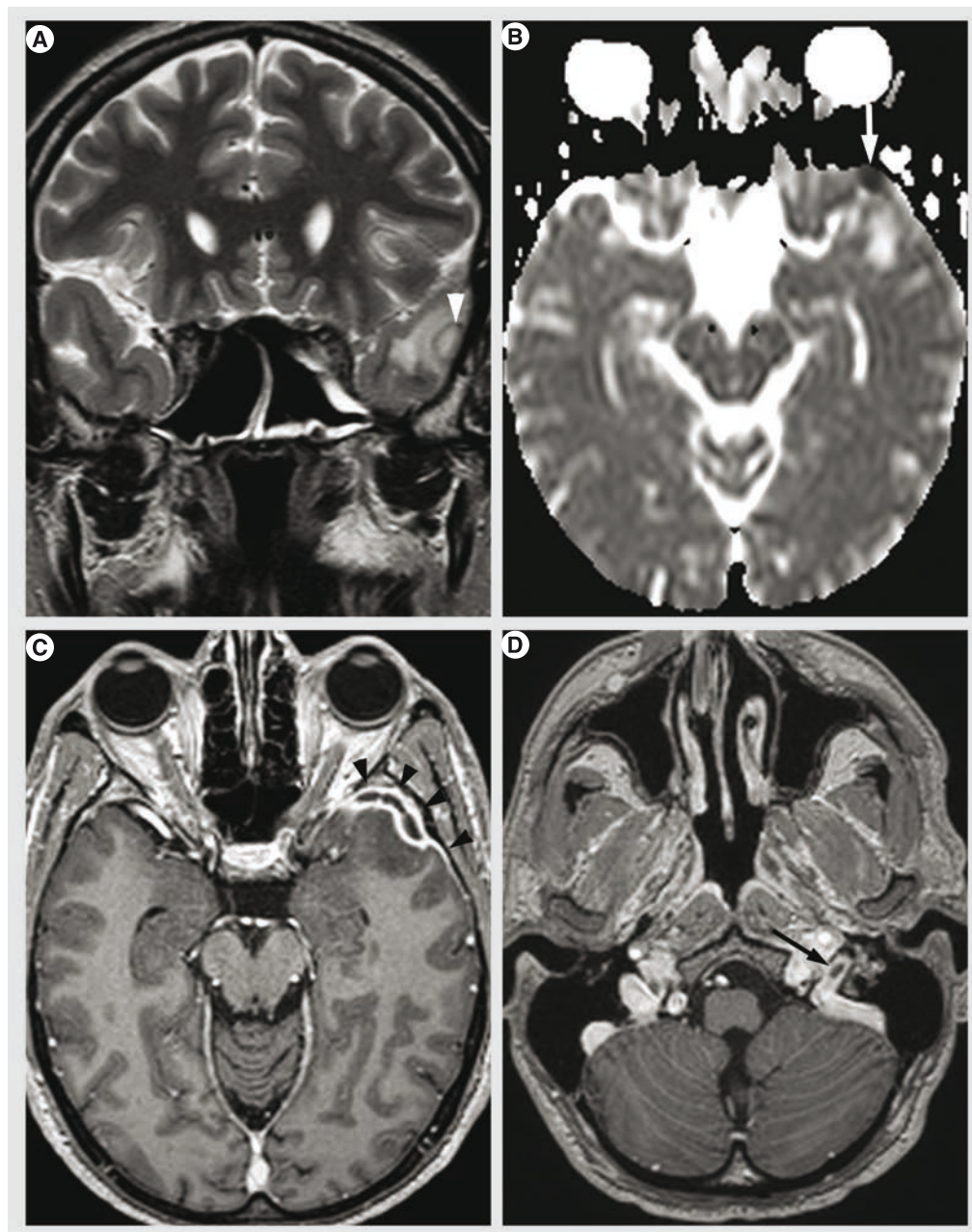


**Figure 10. Subdural empyema and jugular bulb venous thrombosis in a patient with infective endocarditis.** (A) Coronal  $T_2$  showing a small left temporal subdural collection (arrowhead) surrounded by cerebral edema. (B) Axial apparent diffusion coefficient map: the pyogenic content is confirmed by low apparent diffusion coefficient values (arrow). (C) Axial reconstruction of gadolinium-enhanced  $3D T_1$ : peripheral contrast enhancement and dural thickening (arrowheads). (D) Axial reconstruction of gadolinium-enhanced  $3D T_1$ : partial opacification defect in the left jugular bulb (arrow) suggesting venous thrombosis.

encephalopathy syndrome and multifocal leukoencephalopathy [82]. The latter is seen on MR imaging as white matter  $T_2$  hyperintensities ranging from small areas to diffuse lesions, they are hypointense on DWI, have increased ADC and they suggest vasogenic edema due to increased permeability of the blood–brain barrier; they worsen with increased duration of shock and they are associated with poor outcome [83].

#### Posterior reversible encephalopathy syndrome

Posterior reversible encephalopathy syndrome (PRES) is characterized by headache, visual disturbance and/or seizures. MR imaging typically shows bilateral, predominantly posterior vasogenic edema. The mechanism seems to be related to the release of inflammatory cytokines with subsequent endothelial damage and

increased permeability of the blood–brain barrier. PRES in sepsis is more frequent in Gram-positive infections, probably due to the more generalized inflammatory response in this setting. Also, PRES in sepsis is more frequently associated with vascular abnormalities, especially distal reversible vasospasm [84].

#### Acute disseminated encephalomyelitis

Acute disseminated encephalomyelitis (ADEM) is a monophasic inflammatory demyelinating disorder associated with a recent infection or vaccination [2]. Although ADEM is not an infection of the CNS in a strict sense, it is discussed in this context due to overlapping imaging features and usually its parainfectious origin. Its clinical presentation is rather variable, ranging from behavioral disturbances, headaches, vomiting, fever or focal neurological signs to seizures and coma. MR imaging shows multiple, asymmetrically distributed, poorly margined hyperintense lesions on T<sub>2</sub>-weighted and FLAIR images, with variable contrast enhancement; when present, contrast enhancement involves most of the lesions simultaneously [85]. The lesions are found both in white and gray matter; in 30% of cases there is also a spinal cord involvement. The demyelinating origin is suggested by the paucity of the edema and subtle mass effect in comparison to the size of the lesions, incomplete

ring enhancement and decreased rCBV on perfusion [2]. DWI shows restricted diffusion in the acute stage, probably due to the swelling of the myelin sheaths, reduced vascular supply and dense inflammatory cell infiltration, with increased diffusibility in the subacute stage due to axonal loss, demyelination and extracellular edema [85]. MRS is normal in the acute phase, but it can show reduction of NAA and increase of choline in the subacute phase [86]. Main differential diagnosis is MS due to the demyelinating features, but the monophasic evolution, the involvement of deep gray matter and the relative lack of periventricular lesions (Dawson's fingers) are in favor of ADEM [2,85].

### Spinal cord & spinal meninges infections

#### ■ Spinal epidural abscess

Spinal epidural abscess is a rare entity, but of increasing incidence as predisposing factors, such as injected-drug use, aging population, increase of patients with medical comorbidities and spinal surgery, become more common [87,88]. It may occur primarily or complicating infectious spondylodiscitis, osteomyelitis or spinal surgery. Patients generally present with back pain, and other symptoms (fever, neurological dysfunctions) are inconstant. A high index of suspicion is necessary in the initial phases, before

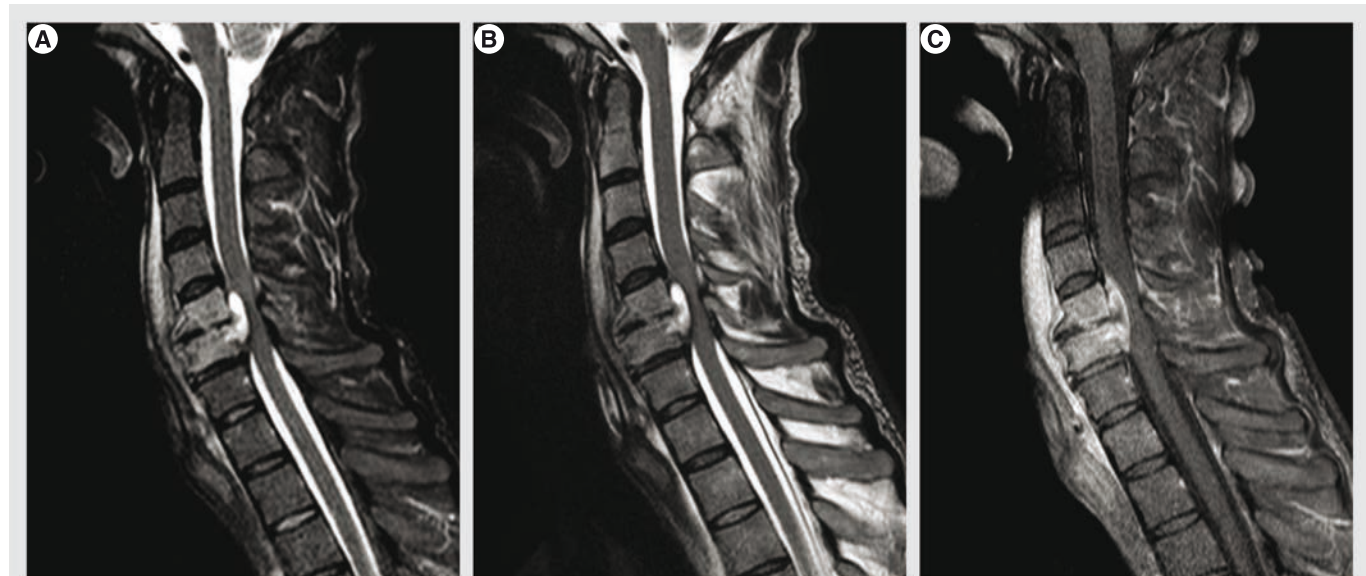


**Figure 11. Spinal epidural abscess complicating C5–C6 bacterial spondylodiscitis. (A)** Sagittal short tau inversion recovery: anterior epidural lesion with hyperintense content and mass effect on the spinal cord; note also the hyperintensities of the medullary bone of C5 and C6 vertebral bodies, discal thinning and prevertebral infiltration. **(B)** Sagittal T<sub>2</sub> showing similar features of the epidural lesion, but the abnormalities of the medullary bone are hardly visible. **(C)** Sagittal contrast-enhanced fat saturated T<sub>1</sub>: the epidural lesion presents a central part without enhancement, in favor of abscess; no abscess in the prevertebral infiltration; slight contrast enhancement of the C5–C6 disc and obvious contrast enhancement of the vertebral bodies. Surgical decompression was performed and *Staphylococcus aureus* was identified in the culture.

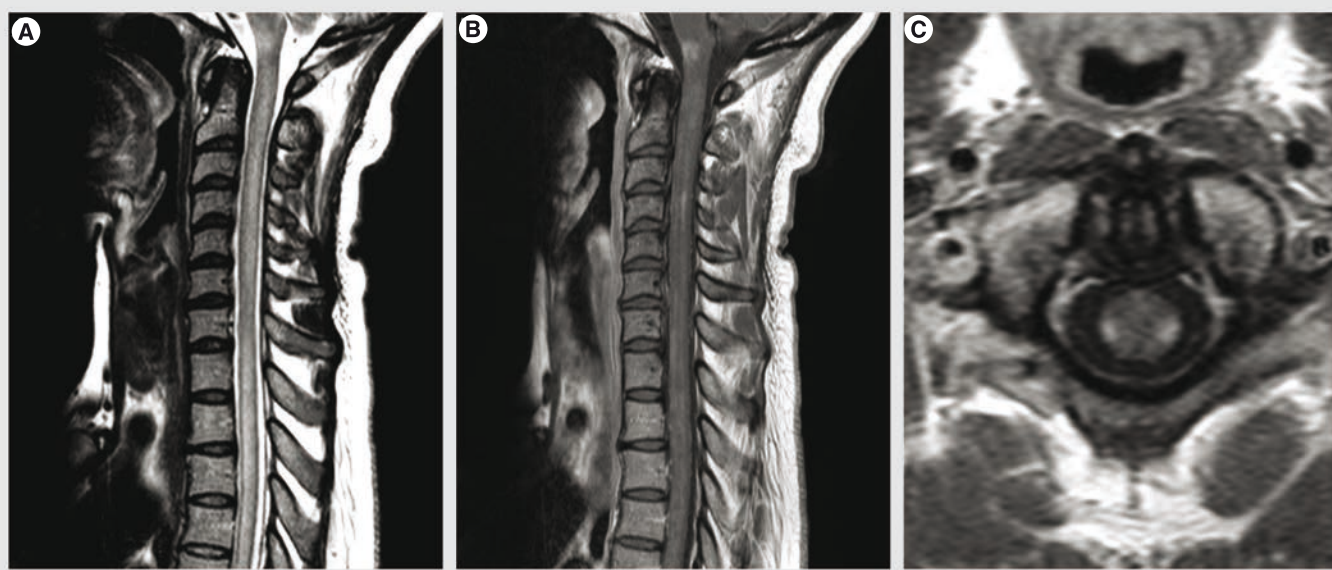


**Figure 12. Viral myelitis with medulla oblongata involvement. (A)** Sagittal  $T_2$ : diffuse hyperintensity in the cervical and upper thoracic spinal cord with slight mass enhancement; note also the involvement of the medulla oblongata. **(B)** Sagittal contrast-enhanced  $T_1$ : patchy and diffuse contrast enhancement. **(C)** Axial contrast-enhanced  $T_1$ : bilateral contrast enhancement of the lateral tracts.

vascular compromise or neural compression causes sudden neurological deterioration. MRI is the modality of choice, showing an epidural collection, isointense or hypointense on  $T_1$ , hyperintense on  $T_2$  with peripheral contrast enhancement (FIGURE 11) [89]. DWI is increasingly used to confirm the pyogenic nature of the content, with restricted diffusion. It is important to look also for other infectious signs that are commonly associated, such as infectious spondylodiscitis or osteomyelitis.

#### ■ Bacterial myelitis & spinal cord abscess

Bacterial myelitis and spinal cord abscess are rare complications of systemic bacteremia. The clinical presentation includes motor and sensory neurological deficits, back pain and fever [90]. Spinal cord abscess formation is similar to its cerebral counterpart, with an initial phase of inflammation (with  $T_2$  hyperintensity and variable contrast enhancement) that gradually becomes encapsulated (with peripheral enhancement and DWI hyperintensity of the content) [91,92].

#### ■ Transverse myelitis

Transverse myelitis is a heterogeneous group of inflammatory disorders characterized by acute or subacute motor, sensory and autonomic spinal cord dysfunction [92]. The most frequent causes are autoimmune phenomena after infection or vaccination, direct infection, autoimmune systemic diseases or acquired demyelinating diseases [93]. MRI is important in the work-up in

order to demonstrate spinal cord inflammation and to eliminate compressive, vascular, metabolic or neoplastic causes. The lesions occupy at least two-thirds of the cross-sectional area of the cord and they span at least two vertebral segments. They are hyperintense on  $T_2$ -weighted sequences, they may enhance in the acute phase with a moderate patchy or diffuse enhancement (FIGURE 12); spinal cord MRI is normal in 40% of cases [90,93]. The extent of the lesions is important for the differential diagnosis, since lesions occupying less than half of the cross-sectional area of the spinal cord and extending less than two vertebral segments are suggestive of MS. DTI seems to be a promising tool for a better characterization of spinal cord involvement and for differential diagnosis, showing increased FA values with decreased ADC in the lesion's periphery, unlike invasive tumors in which FA is low in the periphery or MS myelitis in which ADC is normal or increased in the periphery [90,94].

#### ■ Vacuolar myelopathy

Vacuolar myelopathy is the myelopathy most commonly associated with HIV infection. It is a slowly progressive painless spastic paraparesis, with sensory ataxia and neurogenic bladder, characterized by vacuolar changes in the ascending and descending tracts, particularly in the thoracic spinal cord [95]. It is identified in almost 50% of cases at autopsy, but MRI is frequently normal; when abnormal, it shows imaging features similar to the B12 vitamin deficit, probably due to a similar mechanism [90,95]. It appears as

bilateral T<sub>2</sub> hyperintensities located in the lateral and posterior columns, over multiple spinal cord segments, without contrast enhancement.

### Conclusion

A multitude of infectious agents are responsible for various clinical pictures and imaging features; although this extreme heterogeneity limits the radiological specificity, MR imaging remains an invaluable tool for detection, characterization and follow-up of CNS infections.

### Future perspective

Quantitative imaging (MRS, ADC and FA values derived from diffusion imaging, PWI)

will play an increasing role because it is relatively unbiased, allows for easy comparisons and monitoring and may also detect abnormalities in the seemingly normal CNS.

### Financial & competing interests disclosure

*The authors have no relevant affiliations or financial involvement with any organization or entity with a financial interest in or financial conflict with the subject matter or materials discussed in the manuscript. This includes employment, consultancies, honoraria, stock ownership or options, expert testimony, grants or patents received or pending, or royalties.*

*No writing assistance was utilized in the production of this manuscript.*

### Executive summary

- MR protocol for suspected CNS infection is rather comprehensive, including T<sub>2</sub>, FLAIR, T<sub>2</sub><sup>\*</sup>, diffusion weighted imaging (DWI), diffusion tensor imaging, T<sub>1</sub> without and with gadolinium; in selected cases, gadolinium-enhanced FLAIR, MR angiography, MR perfusion and spectroscopy may be added.
  - Various imaging patterns are encountered in brain infections: extra-axial lesion, ring enhancing lesion, temporal lobe lesion, basal ganglia lesion and white matter abnormality.
  - Extra-axial collections have DWI hyperintensity; leptomeningeal involvement is best seen on FLAIR sequence, especially gadolinium enhanced.
  - Ring enhancing lesions: the central part of the pyogenic abscesses has diffusion restriction, but care for mimics (hematomas, some metastasis); do not forget that not all infectious cysts are pyogenic (e.g., toxoplasmosis, granulomas and cysticercosis); in immunocompromised patients, consider toxoplasmosis (therapy test, hypovascular) versus lymphoma (hypervascular).
  - Temporal lobe lesion: acutely presenting, but nonvascular DWI hyperintensity – consider herpes simplex encephalitis; visualization of hemorrhage is rare, but important for differentiating it from paraneoplastic limbic encephalitis or epileptic seizure.
  - Basal ganglia lesion: bilateral lesions involving the entire basal ganglia: consider systemic or metabolic origin; unilateral, asymmetrical or focal lesions: probably infection or neoplasm; bilateral DWI hyperintensity in demented patient: Creutzfeldt–Jakob disease; rapidly enlarging cysts in immunocompromised patient: cryptococcosis.
  - White matter lesion: HIV encephalopathy (periventricular T<sub>2</sub> hyperintensity, T<sub>1</sub> isointensity, increased water diffusion) versus progressive multifocal leukoencephalopathy (subcortical U fibers, T<sub>1</sub> hypointensity, DWI hyperintense advancing rim).
- In immunocompromised patients, beware of co-infections and IRIS.
- Spinal epidural abscesses are often complications of other local pathologies (infectious spondylodiscitis and osteomyelitis).

### References

Papers of special note have been highlighted as:

- of interest
- of considerable interest

- 1 Gasparetto EL, Cabral RF, Da Cruz LC Jr, Domingues RC. Diffusion imaging in brain infections. *Neuroimag. Clin. N. Am.* 21(1), 89–113 (2011).
- 2 Aiken AH. Central nervous system infection. *Neuroimag. Clin. N. Am.* 20(4), 557–580 (2010).
- **Excellent review of CNS infections.**
- 3 Kremer S, Abu Eid M, Bierry G *et al.* Accuracy of delayed post-contrast FLAIR MR imaging for the diagnosis of leptomeningeal infectious or tumoral diseases. *J. Neuroradiol.* 33(5), 285–291 (2006).
- 4 Cuvinciuc V, Viguier A, Calviere L *et al.* Isolated acute nontraumatic cortical subarachnoid hemorrhage. *Am. J. Neuroradiol.* 31(8), 1355–1362 (2010).
- 5 Mathews VP, Caldemeyer KS, Lowe MJ, Greenspan SL, Weber DM, Ulmer JL. Brain: gadolinium-enhanced fast fluid-attenuated inversion-recovery MR imaging. *Radiology* 211(1), 257–263 (1999).
- 6 Splendiani A, Puglielli E, De Amicis R, Necozone S, Masciocchi C, Gallucci M. Contrast-enhanced FLAIR in the early diagnosis of infectious meningitis. *Neuroradiology* 47(8), 591–598 (2005).
- 7 Smirniotopoulos JG, Murphy FM, Rushing EJ, Rees JH, Schroeder JW. Patterns of contrast enhancement in the brain and meninges. *Radiographics* 27(2), 525–551 (2007).
- **Excellent review that explains the mechanisms of contrast enhancement and its use in the differential diagnosis.**
- 8 Hildenbrand P, Craven DE, Jones R, Nemeskal P. Lyme neuroborreliosis: manifestations of a rapidly emerging zoonosis. *Am. J. Neuroradiol.* 30(6), 1079–1087 (2009).
- 9 Albayram S, Asik M, Hasiloglu ZI, Dikici AS, Erdemli HE, Altintas A. Pathological contrast enhancement of the oculomotor and trigeminal nerves caused by intracranial hypotension syndrome. *Headache* 51(5), 804–808 (2011).
- 10 Santhosh K, Kesavadas C, Thomas B, Gupta AK, Thamburaj K, Kapilamoorthy TR. Susceptibility weighted imaging: a new tool in magnetic resonance imaging of stroke. *Clin. Radiol.* 64(1), 74–83 (2009).
- 11 Devere G, Andrew M, Adams C *et al.* Cerebral sinovenous thrombosis in children. *N. Engl. J. Med.* 345(6), 417–423 (2001).
- 12 Hyare H, Thornton J, Stevens J *et al.* High-b-value diffusion MR imaging and basal nuclei apparent diffusion coefficient measurements in variant and sporadic

- Creutzfeldt-Jakob disease. *Am. J. Neuroradiol.* 31(3), 521–526 (2010).
- 13 Stadnik TW, Chaskis C, Michotte A *et al.* Diffusion-weighted MR imaging of intracerebral masses: comparison with conventional MR imaging and histologic findings. *Am. J. Neuroradiol.* 22(5), 969–976 (2001).
- 14 Bergui M, Bradac GB, Oguz KK *et al.* Progressive multifocal leukoencephalopathy: diffusion-weighted imaging and pathological correlations. *Neuroradiology* 46(1), 22–25 (2004).
- 15 Mittal S, Farmer P, Kalina P, Kingsley PB, Halperin J. Correlation of diffusion-weighted magnetic resonance imaging with neuropathology in Creutzfeldt-Jakob disease. *Arch. Neurol.* 59(1), 128–134 (2002).
- 16 Filippi CG, Ulug AM, Ryan E, Ferrando SJ, Van Gorp W. Diffusion tensor imaging of patients with HIV and normal-appearing white matter on MR images of the brain. *Am. J. Neuroradiol.* 22(2), 277–283 (2001).
- 17 Stebbins GT, Smith CA, Bartt RE *et al.* HIV-associated alterations in normal-appearing white matter: a voxel-wise diffusion tensor imaging study. *J. Acquir. Immune Defic. Syndr.* 46(5), 564–573 (2007).
- 18 Trivedi R, Gupta RK, Agarwal A *et al.* Assessment of white matter damage in subacute sclerosing panencephalitis using quantitative diffusion tensor MR imaging. *Am. J. Neuroradiol.* 27(8), 1712–1716 (2006).
- 19 Trivedi R, Anuradha H, Agarwal A *et al.* Correlation of quantitative diffusion tensor tractography with clinical grades of subacute sclerosing panencephalitis. *Am. J. Neuroradiol.* 32(4), 714–720 (2011).
- 20 Lacerda S, Law M. Magnetic resonance perfusion and permeability imaging in brain tumors. *Neuroimag. Clin. N. Am.* 19(4), 527–557 (2009).
- 21 Sourbron S. Technical aspects of MR perfusion. *Eur. J. Radiol.* 76(3), 304–313 (2010).
- 22 Jarnum H, Steffensen EG, Knutsson L *et al.* Perfusion MRI of brain tumours: a comparative study of pseudo-continuous arterial spin labelling and dynamic susceptibility contrast imaging. *Neuroradiology* 52(4), 307–317 (2010).
- 23 Kingsley PB, Shah TC, Woldenberg R. Identification of diffuse and focal brain lesions by clinical magnetic resonance spectroscopy. *NMR Biomed.* 19(4), 435–462 (2006).
- 24 Lai PH, Hsu SS, Ding SW *et al.* Proton magnetic resonance spectroscopy and diffusion-weighted imaging in intracranial cystic mass lesions. *Surg. Neurol.* 68 (Suppl. 1), S25–S36 (2007).
- 25 Khanna PC, Godinho S, Patkar DP, Pungavkar SA, Lawande MA. MR spectroscopy-aided differentiation: “giant” extra-axial tuberculoma masquerading as meningioma. *Am. J. Neuroradiol.* 27(7), 1438–1440 (2006).
- 26 Hoxworth JM, Glastonbury CM. Orbital and intracranial complications of acute sinusitis. *Neuroimag. Clin. N. Am.* 20(4), 511–526 (2010).
- 27 Reiche W, Schuchardt V, Hagen T, Il'yasov KA, Billmann P, Weber J. Differential diagnosis of intracranial ring enhancing cystic mass lesions – role of diffusion-weighted imaging (DWI) and diffusion-tensor imaging (DTI). *Clin. Neurol. Neurosurg.* 112(3), 218–225 (2010).
- 28 Blasel S, Jurcoane A, Franz K, Morawe G, Pellikan S, Hattingen E. Elevated peritumoural rCBV values as a mean to differentiate metastases from high-grade gliomas. *Acta. Neurochir. (Wien)* 152(11), 1893–1899 (2010).
- 29 Fan G, Sun B, Wu Z, Guo Q, Guo Y. *In vivo* single-voxel proton MR spectroscopy in the differentiation of high-grade gliomas and solitary metastases. *Clin. Radiol.* 59(1), 77–85 (2004).
- 30 Hegde AN, Mohan S, Lath N, Lim CC. Differential diagnosis for bilateral abnormalities of the basal ganglia and thalamus. *Radiographics* 31(1), 5–30 (2011).
- 31 Mathisen GE, Johnson JP. Brain abscess. *Clin. Infect. Dis.* 25(4), 763–779; quiz 780–761 (1997).
- 32 Hughes DC, Raghavan A, Mordekar SR, Griffiths PD, Connolly DJ. Role of imaging in the diagnosis of acute bacterial meningitis and its complications. *Postgrad. Med. J.* 86(1018), 478–485 (2010).
- 33 Haimes AB, Zimmerman RD, Morgello S *et al.* MR imaging of brain abscesses. *Am. J. Roentgenol.* 152(5), 1073–1085 (1989).
- 34 Rhode V, Van Oosterhout A, Mull M, Gilsbach JM. Subarachnoid haemorrhage as initial symptom of multiple brain abscesses. *Acta. Neurochir. (Wien)* 142(2), 205–208 (2000).
- 35 Rumboldt Z, Thurnher MM, Gupta RK. Central nervous system infections. *Semin. Roentgenol.* 42(2), 62–91 (2007).
- **Excellent review of CNS infections.**
- 36 Holtas S, Geijer B, Stromblad LG, Maly-Sundgren P, Burtscher IM. A ring-enhancing metastasis with central high signal on diffusion-weighted imaging and low apparent diffusion coefficients. *Neuroradiology* 42(11), 824–827 (2000).
- 37 Nath K, Agarwal M, Ramola M *et al.* Role of diffusion tensor imaging metrics and *in vivo* proton magnetic resonance spectroscopy in the differential diagnosis of cystic intracranial mass lesions. *Magn. Reson. Imag.* 27(2), 198–206 (2009).
- 38 Cartes-Zumelzu FW, Stavrou I, Castillo M, Eisenhuber E, Knosp E, Thurnher MM. Diffusion-weighted imaging in the assessment of brain abscesses therapy. *Am. J. Neuroradiol.* 25(8), 1310–1317 (2004).
- 39 Burtscher IM, Holtas S. *In vivo* proton MR spectroscopy of untreated and treated brain abscesses. *Am. J. Neuroradiol.* 20(6), 1049–1053 (1999).
- 40 Holmes TM, Petrella JR, Provenzale JM. Distinction between cerebral abscesses and high-grade neoplasms by dynamic susceptibility contrast perfusion MRI. *Am. J. Roentgenol.* 183(5), 1247–1252 (2004).
- 41 Smith AB, Smirniotopoulos JG, Rushing EJ. From the archives of the AFIP: central nervous system infections associated with human immunodeficiency virus infection: radiologic-pathologic correlation. *Radiographics* 28(7), 2033–2058 (2008).
- 42 Gupta RK, Vatsal DK, Husain N *et al.* Differentiation of tuberculous from pyogenic brain abscesses with *in vivo* proton MR spectroscopy and magnetization transfer MR imaging. *Am. J. Neuroradiol.* 22(8), 1503–1509 (2001).
- 43 Lyme disease – United States, 2003–2005. *MMWR Morb. Mortal. Wkly. Rep.* 56(23), 573–576 (2007).
- 44 Agosta F, Rocca MA, Benedetti B, Capra R, Cordioli C, Filippi M. MR imaging assessment of brain and cervical cord damage in patients with neuroborreliosis. *Am. J. Neuroradiol.* 27(4), 892–894 (2006).
- 45 Andreula C. Cranial viral infections in the adult. *Eur. Radiol.* 14 (Suppl. 3), E132–E144 (2004).
- 46 Vargas MI, Pereira VM, Haller S *et al.* Magnetic resonance imaging of infections of the white matter. *Top Magn. Reson. Imag.* 20(6), 325–331 (2009).
- 47 Bulakbasi N, Kocaoglu M. Central nervous system infections of herpesvirus family. *Neuroimag. Clin. N. Am.* 18(1), 53–84 (2008).
- 48 Demaerel P, Wilms G, Robberecht W *et al.* MRI of herpes simplex encephalitis. *Neuroradiology* 34(6), 490–493 (1992).
- 49 Sawlani V. Diffusion-weighted imaging and apparent diffusion coefficient evaluation of herpes simplex encephalitis and Japanese encephalitis. *J. Neurol. Sci.* 287(1–2), 221–226 (2009).
- 50 Herweh C, Jayachandra MR, Hartmann M *et al.* Quantitative diffusion tensor

- imaging in herpes simplex virus encephalitis. *J. Neurovirol.* 13(5), 426–432 (2007).
- 51 Cha S, Knopp EA, Johnson G, Wetzel SG, Litt AW, Zagzag D. Intracranial mass lesions: dynamic contrast-enhanced susceptibility-weighted echo-planar perfusion MR imaging. *Radiology* 223(1), 11–29 (2002).
- 52 Misra UK, Tan CT, Kalita J. Viral encephalitis and epilepsy. *Epilepsia* 49 (Suppl. 6), 13–18 (2008).
- 53 Handique SK, Das RR, Barman K *et al.* Temporal lobe involvement in Japanese encephalitis: problems in differential diagnosis. *Am. J. Neuroradiol.* 27(5), 1027–1031 (2006).
- 54 Thurnher MM, Sundgren PC. Imaging of slow viruses. *Neuroimag. Clin. of N. Am.* 18(1), 133–148; ix (2008).
- 55 Aydin K, Okur O, Tatli B, Sarwar SG, Ozturk C, Dilber C. Reduced gray matter volume in the frontotemporal cortex of patients with early subacute sclerosing panencephalitis. *Am. J. Neuroradiol.* 30(2), 271–275 (2009).
- 56 Alkan A, Korkmaz L, Sigirci A *et al.* Subacute sclerosing panencephalitis: relationship between clinical stage and diffusion-weighted imaging findings. *J. Magn. Reson. Imag.* 23(3), 267–272 (2006).
- 57 Amend KL, Turnbull B, Foskett N, Napalkov P, Kurth T, Seeger J. Incidence of progressive multifocal leukoencephalopathy in patients without HIV. *Neurology* 75(15), 1326–1332 (2010).
- 58 Shah R, Bag AK, Chapman PR, Cure JK. Imaging manifestations of progressive multifocal leukoencephalopathy. *Clin. Radiol.* 65(6), 431–439 (2010).
- 59 Yoon JH, Bang OY, Kim HS. Progressive multifocal leukoencephalopathy in AIDS: Proton MR spectroscopy patterns of asynchronous lesions confirmed by serial diffusion-weighted imaging and apparent diffusion coefficient mapping. *J. Clin. Neurol.* 3(4), 200–203 (2007).
- 60 Ramsey RG, Gean AD. Neuroimaging of AIDS. I. Central nervous system toxoplasmosis. *Neuroimag. Clin. N. Am.* 7(2), 171–186 (1997).
- 61 Young RJ, Ghesani MV, Kagetsu NJ, Derogatis AJ. Lesion size determines accuracy of thallium-201 brain single-photon emission tomography in differentiating between intracranial malignancy and infection in AIDS patients. *Am. J. Neuroradiol.* 26(8), 1973–1979 (2005).
- 62 Ernst TM, Chang L, Witt MD *et al.* Cerebral toxoplasmosis and lymphoma in AIDS: perfusion MR imaging experience in 13 patients. *Radiology* 208(3), 663–669 (1998).
- 63 Schroeder PC, Post MJ, Oschatz E, Stadler A, Bruce-Gregorios J, Thurnher MM. Analysis of the utility of diffusion-weighted MRI and apparent diffusion coefficient values in distinguishing central nervous system toxoplasmosis from lymphoma. *Neuroradiology* 48(10), 715–720 (2006).
- 64 Yeane GA, Kolar BS, Silberstein HJ, Wang HZ. Case 163: solitary neurocysticercosis. *Radiology* 257(2), 581–585 (2010).
- 65 Braga F, Rocha AJ, Gomes HR, Filho GH, Silva CJ, Fonseca RB. Noninvasive MR cisternography with fluid-attenuated inversion recovery and 100% supplemental O(2) in the evaluation of neurocysticercosis. *Am. J. Neuroradiol.* 25(2), 295–297 (2004).
- 66 Andreula CF, Burdi N, Carella A. CNS cryptococcosis in AIDS: spectrum of MR findings. *J. Comput. Assist. Tomogr.* 17(3), 438–441 (1993).
- 67 Almutairi BM, Nguyen TB, Jansen GH, Asseri AH. Invasive aspergillosis of the brain: radiologic-pathologic correlation. *Radiographics* 29(2), 375–379 (2009).
- 68 Zinreich SJ, Kennedy DW, Malat J *et al.* Fungal sinusitis: diagnosis with CT and MR imaging. *Radiology* 169(2), 439–444 (1988).
- 69 Oner AY, Celik H, Akpek S, Tokgoz N. Central nervous system aspergillosis: magnetic resonance imaging, diffusion-weighted imaging, and magnetic resonance spectroscopy features. *Acta Radiol.* 47(4), 408–412 (2006).
- 70 Du Plessis DG. Prion protein disease and neuropathology of prion disease. *Neuroimag. Clin. N. Am.* 18(1), 163–182; ix (2008).
- 71 Mendonca RA, Martins G, Lugokenski R, Rossi MD. Subacute spongiform encephalopathies. *Top Magn. Reson. Imag.* 16(2), 213–219 (2005).
- 72 Yung B, Moeller JJ, Bitar M, Chong D. Teaching NeuroImages: hemispheric-onset Creutzfeldt-Jakob disease with concordant MRI and EEG findings. *Neurology* 75(16), e66 (2010).
- 73 Chohan G, Pennington C, Mackenzie JM *et al.* The role of cerebrospinal fluid 14-3-3 and other proteins in the diagnosis of sporadic Creutzfeldt-Jakob disease in the UK: a 10-year review. *J. Neurol. Neurosurg. Psychiatry* 81(11), 1243–1248 (2010).
- 74 Young GS, Geschwind MD, Fischbein NJ *et al.* Diffusion-weighted and fluid-attenuated inversion recovery imaging in Creutzfeldt-Jakob disease: high sensitivity and specificity for diagnosis. *Am. J. Neuroradiol.* 26(6), 1551–1562 (2005).
- 75 Maroba M, Tonami H, Miyaji H, Yokota H, Yamamoto I. Creutzfeldt-Jakob disease: serial changes on diffusion-weighted MRI. *J. Comput. Assist. Tomogr.* 25(2), 274–277 (2001).
- 76 Straus SE, Thorpe KE, Holroyd-Leduc J. How do I perform a lumbar puncture and analyze the results to diagnose bacterial meningitis? *JAMA* 296(16), 2012–2022 (2006).
- 77 Wong AM, Zimmerman RA, Simon EM, Pollock AN, Bilaniuk LT. Diffusion-weighted MR imaging of subdural empyemas in children. *Am. J. Neuroradiol.* 25(6), 1016–1021 (2004).
- 78 Martin-Blondel G, Delobel P, Blancher A *et al.* Pathogenesis of the immune reconstitution inflammatory syndrome affecting the central nervous system in patients infected with HIV. *Brain* 134(Pt 4), 928–946 (2011).
- **An excellent insight into the pathogenesis of a fascinating iatrogenic ‘complication’.**
- 79 Buckle C, Castillo M. Use of diffusion-weighted imaging to evaluate the initial response of progressive multifocal leukoencephalopathy to highly active antiretroviral therapy: early experience. *Am. J. Neuroradiol.* 31(6), 1031–1035 (2010).
- 80 Cuvinciu V, Martin-Blondel G, Marchou B, Bonneville F. Proton MR spectroscopy of progressive multifocal leukoencephalopathy-immune reconstitution inflammatory syndrome. *Am. J. Neuroradiol.* 31(8), E69–E70; author reply E71 (2010).
- 81 Azuma A, Toyoda K, O’uchi T. Brain magnetic resonance findings in infective endocarditis with neurological complications. *Jpn. J. Radiol.* 27(3), 123–130 (2009).
- 82 Burkhart CS, Siegemund M, Steiner LA. Cerebral perfusion in sepsis. *Crit. Care.* 14(2), 215 (2010).
- 83 Sharshar T, Carlier R, Bernard F *et al.* Brain lesions in septic shock: a magnetic resonance imaging study. *Intensive Care Med.* 33(5), 798–806 (2007).
- 84 Bartynski WS, Boardman JF, Zeigler ZR, Shaddock RK, Lister J. Posterior reversible encephalopathy syndrome in infection, sepsis, and shock. *Am. J. Neuroradiol.* 27(10), 2179–2190 (2006).
- 85 Rossi A. Imaging of acute disseminated encephalomyelitis. *Neuroimag. Clin. N. Am.* 18(1), 149–161; ix (2008).
- 86 Balasubramanya KS, Kovoov JM, Jayakumar PN *et al.* Diffusion-weighted imaging and proton MR spectroscopy in the characterization of acute disseminated encephalomyelitis. *Neuroradiology* 49(2), 177–183 (2007).
- 87 Wang VY, Chou D, Chin C. Spine and spinal cord emergencies: vascular and

- infectious causes. *Neuroimag. Clin. N. Am.* 20(4), 639–650 (2010).
- 88 Pradilla G, Ardila GP, Hsu W, Rigamonti D. Epidural abscesses of the CNS. *Lancet Neurol.* 8(3), 292–300 (2009).
- 89 Curry WT, Jr, Hoh BL, Amin-Hanjani S, Eskandar EN. Spinal epidural abscess: clinical presentation, management, and outcome. *Surg. Neurol.* 63(4), 364–371; discussion 371 (2005).
- 90 Thurnher MM, Cartes-Zumelzu F, Mueller-Mang C. Demyelinating and infectious diseases of the spinal cord. *Neuroimag. Clin. N. Am.* 17(1), 37–55 (2007).
- 91 Murphy KJ, Brunberg JA, Quint DJ, Kazanjian PH. Spinal cord infection: myelitis and abscess formation. *Am. J. Neuroradiol.* 19(2), 341–348 (1998).
- 92 Proposed diagnostic criteria and nosology of acute transverse myelitis. *Neurology* 59(4), 499–505 (2002).
- 93 Frohman EM, Wingerchuk DM. Clinical practice. Transverse myelitis. *N. Engl. J. Med.* 363(6), 564–572 (2010).
- 94 Renoux J, Facon D, Fillard P, Huynh I, Lasjaunias P, Ducreux D. MR diffusion tensor imaging and fiber tracking in inflammatory diseases of the spinal cord. *Am. J. Neuroradiol.* 27(9), 1947–1951 (2006).
- 95 McArthur JC, Brew BJ, Nath A. Neurological complications of HIV infection. *Lancet Neurol.* 4(9), 543–555 (2005).